Application of Modern NMR Spectroscopic Techniques to Structural Studies of Wood and Pulp Components

Tiina Liitiä

Laboratory of Polymer Chemistry
Department of Chemistry
University of Helsinki
Helsinki, Finland

ACADEMIC DISSERTATION
FOR THE DEGREE OF DOCTOR OF PHILOSOPHY

To be presented with the permission of the Faculty of Science of the University of Helsinki for public criticism in Auditorium A110 of the Department of Chemistry, A.I. Virtasen aukio 1 on August the 23rd, 2002, at 12 o'clock.

Helsinki 2002

Opponent

Doctor Roger Newman
Industrial Research Limited
Lower Hutt, New Zealand

Reviewers

Professor Tapani Vuorinen
Department of Forest Products Technology
Helsinki University of Technology
Finland

&

Doctor Tomas Larsson
Swedish Pulp and Paper Research Institute, STFI
Stockholm, Sweden

ISBN 952-91-4828-3 (print)
ISBN 952-10-0611-0 (pdf)
http://ethesis.helsinki.fi
Helsinki 2002
Yliopistopaino

PREFACE

The work described in this thesis was carried out at the Laboratory of Polymer Chemistry, University of Helsinki during the years 1997-2002 and it was performed in close collaboration with the Finnish Pulp and Paper Research Institute, KCL.

First of all I wish to express my deepest gratitude to my supervisors Docent Sirkka Liisa Maunu and Docent Bo Hortling for their guidance, encouragement and patience throughout this research. Owing to the very warm and friendly atmosphere, it has been a pleasure to work and to grow as a scientist with them.

I am also grateful to the Head of the Laboratory, Professor Heikki Tenhu and Professor Emerita Franciska Sundholm for the possibility to work in their laboratory and for providing the excellent working facilities.

I wish to thank all the people I have collaborated during these years, but above all I would like to thank Professor Ilkka Kilpeläinen, M.Sc. Merja Toikka, Dr. Jussi Sipilä, Dr. Eva-Lena Hult and Professor Tommy Iversen for their help and contribution to this work. Dr. Tarja Tamminen and Dr. Petteri Malkavaara are also acknowledged for co-operation.

I wish to thank all members of the Laboratory of Polymer Chemistry for creating such a pleasant and friendly working environment. Especially I am grateful to Hanne Sivonen and Tiina Lilja for their friendship and Maria Tahvanainen for bearing me as a roommate. I would also like to thank Heljä Heikkilä, Juha Solasaari and Marjut Wallner for their valuable help whenever needed. Special thanks are due to Dr. Sami Hietala for his assistance with computers and computational problems related to NMR spectroscopy.

My deepest gratitude I owe to my family and friends for their endless love, encouragement and belief in me. Especially I owe sincere thanks to my dearest friend Hannamari for standing by me throughout the years, and making also the rough times more bearable.

The National Technology Agency of Finland (TEKES) is greatly acknowledged for financing of this study, which was carried out under the Wood Wisdom research programme. The Oscar Öflund Foundation, The Foundation of Technology and the Magnus Ehrnrooth Foundation are also acknowledged.

Helsinki, 2002

Tiina Liitiä

ABSTRACT

Various NMR spectroscopic techniques in both solid and liquid state were applied to investigate the polymeric components of wood and pulp. The aim of the work was to obtain new structural information on the changes occurring in the morphology of cellulose and in the lignin structure during various chemical pulping related processes in order to help optimising the conditions for efficient delignification and bleaching reactions without compromising pulp yield or strength properties. Mainly the effects of kraft pulping and oxygen delignification were investigated, but some samples of sulphite, PS-AQ and soda-AQ pulping were also studied. One of the main objectives of this research was to investigate if some parts of the spruce fibre are affected unequally by kraft pulping. Therefore, the residual lignin structure and the crystallinity of cellulose in ray cells and on the fibre surface were compared to the corresponding structures inside the fibre by isolating fines fractions before and after refining of kraft pulp. Mainly softwood components were considered throughout this thesis.

According to the ^{13}C CPMAS measurements the crystallinity of cellulose increases during pulping and the metastable cellulose I_α is converted to the more stable cellulose I_β polymorph. Various pulping methods or hemicellulose contents were not, however, observed to affect cellulose crystallinity. A slightly lower degree of cellulose crystallinity was found in birch pulps compared to the corresponding pine pulps, and the birch pulps were also assumed to contain larger amounts of well-ordered xylan. After kraft pulping, cellulose crystallinity was found lower in ray cells and on the fibre surface compared to the long fibre fractions. Refining was observed slightly to facilitate the cellulose crystallization as well as the cellulose fibril aggregation during drying due to the better swellability of the fibres. A slight increase in cellulose crystallinity during oxygen delignification was also observed, whereas during the QPZP-bleaching sequence the degree of cellulose crystallinity decreased slightly.

The results of ^{13}C CPMAS as well as 2D HSQC and 3D HSQC-TOCSY measurements show that most of the original structures identified in MWL are still present in technical lignins, although their relative proportions vary after kraft pulping and oxygen delignification. The cleavage of aryl ether linkages during kraft pulping and the preserving effect of oxygen delignification on aryl ether linkages were observed in both solid state and in solution NMR studies. However, some reactive structures, e.g. β-O-4 and dibenzodioxocin structures were still found in residual lignin after kraft pulping and some of the reactive structures were shown to survive even in the dissolved spent liquor lignin. Similarly, residual lignin is still to a certain extent phenolic after oxygen delignification. The reactivity of those functionalities may thus be hindered by their involvement with less reactive condensed structures or LC-complexes. According to the dipolar dephasing measurements, the condensed aromatic lignin structures were found to enrich into fibres during pulping and oxygen delignification, whereas the less condensed lignin structures were removed already in the early stage of pulping. However, condensed diphenyl methane structures supposed to be formed in kraft pulping conditions, could not be found in the residual lignins. Evidence of residual lignin-carbohydrate complexes was obtained indirectly by ordinary ^{13}C CPMAS measurements as well as by proton spin-lattice relaxation measurements. According to these results, interactions between cellulose and lignin are possible. In ray cells and on the fibre surface the suggested interactions are more prominent than in the fibres. Otherwise, no significant differences in residual lignin structure between fines and long fibres were observed. Residual

lignin of fines was found to be less phenolic and only very slightly more condensed than the residual lignin of long fibres.

ABBREVIATIONS

1D	one-dimensional
2D	two-dimensional
3D	three-dimensional
AH	acid hydrolysis
AQ	anthraquinone
CPMAS	cross-polarization magic angle spinning
D	chlorine dioxide
DEPT	distortionless enhancement by polarization transfer
DL	delignification
DPM	diphenyl methane
E	extraction
ECF	elemental chlorine free
EDTA	ethylenediaminetetraacetic acid
FID	free induction decay
FT	flow-through
H	sodium hypochlorite
HETCOR	heterocorrelation spectroscopy
HMBC	heteronuclear multiple bond correlation spectroscopy
HSQC	heteronuclear single quantum correlation spectroscopy
RLCC	residual lignin-carbohydrate complex
LCC	lignin-carbohydrate complex
LC	lignin-carbohydrate
LFD	lateral fibril dimension
LFAD	lateral fibril aggregate dimension
MWL	milled wood lignin
NMR	nuclear magnetic resonance
O	oxygen
P	hydrogen peroxide
PEO-*co*-PPO	poly(ethylene oxide-*co*-propylene oxide)
PS	polysulphide
PSRE	proton spin-relaxation based spectral edition
Q	chelation
RL	residual lignin
SLL	spent liquor lignin
TCF	total chlorine free
TOCSY	total correlation spectroscopy
X	xylanase
Z	ozone

SYMBOLS

CH_{number}	number of protonated carbons
CrI	crystallinity index
f^H	fraction of protonated carbons
I^0_a	initial intensity of protonated aromatic carbons
I_a	intensity of protonated aromatic carbons
I^0_b	initial intensity of non-protonated aromatic carbons
I_b	intensity of non-protonated aromatic carbons
I_{tot}	total intensity of protonated and non-protonated aromatic carbons
T_{1H}	proton spin-lattice relaxation time
$T_{1\rho H}$	proton spin-lattice relaxation time in a rotating frame
T'_{2a}	decay constant of protonated aromatic carbons
T'_{2b}	decay constant of non-protonated aromatic carbons
T_{d2}	d2-delay time
t_{90}	90º proton preparation pulse
t_{cntct}	contact time
t_{sl}	spin-lock delay

LIST OF ORIGINAL PUBLICATIONS

This thesis is based on the following seven articles, hereafter referred to in the text by their Roman numerals (I-VII), and some previously unpublished results are also included.

I Maunu, S., Liitiä, T., Kauliomäki, S., Hortling, B. and Sundquist, J., ^{13}C CPMAS NMR investigations of cellulose polymorphs in different pulps, *Cellulose* **7** (2000) 147-159.

II Liitiä, T., Maunu, S.L. and Hortling, B., Solid state NMR studies on cellulose crystallinity in fines and bulk fibres separated from refined kraft pulp, *Holzforschung* **54** (2000) 618-624.

III Liitiä, T., Maunu, S.L. and Hortling, B., Solid state NMR studies on inhomogeneous structure of fibre wall in kraft pulp, *Holzforschung* **55** (2001) 503-510.

IV Hult, E.-L., Liitiä, T., Maunu, S.L. Hortling, B. and Iversen, T., A CP/MAS ^{13}C-NMR study of cellulose structure on the surface of kraft pulp fibers, *Carbohydr. Polym.* **49** (2002) 231-234.

V Liitiä, T., Maunu, S.L. and Hortling, B., Solid-state NMR studies of residual lignin and its association with carbohydrates, *J. Pulp Pap. Sci.* **26** (2000) 323-330.

VI Liitiä, T., Maunu, S.L., Sipilä, J. and Hortling, B., Application of solid-state ^{13}C NMR spectroscopy and dipolar dephasing technique to determine the extent of condensation in technical lignins, *Solid State NMR* **21** (2002) 171-186.

VII Liitiä, T., Maunu, S.L., Hortling, B., Toikka, M. and Kilpeläinen, I., Analysis of technical lignins by two- and three-dimensional NMR spectroscopy, *J. Agric. Food Chem*., accepted.

CONTENTS

1. INTRODUCTION

Growing environmental concern has forced the modern pulp and paper industry to seek more selective and environmentally friendly pulping and bleaching procedures. This has led for example to the preferential utilisation of elemental chlorine free (ECF) and total chlorine free (TCF) bleaching sequences instead of traditional chlorine bleaching. In those bleaching sequences oxygen delignification is a very important stage because of its many environmental and economical benefits. However, due to its limited selectivity the reaction conditions of oxygen delignification still need optimisation.[1] The better understanding of the structure and morphological distribution of not only residual lignin, but all wood components, may aid in optimising conditions for efficient delignification and bleaching reactions without compromising pulp yield or strength properties. Therefore, much effort has been focused on the thorough structural investigation of residual lignin, as well as the other wood components, of unbleached and bleached pulps.

1.1. Chemical pulping

The layered ultrastructure of wood cell is complex. The main component of wood is linear and semicrystalline cellulose, which exists in the form of microfibrils thus providing the 'skeleton', which is surrounded by amorphous hemicelluloses and lignin functioning as matrix and encrusting substances.[1,2] In chemical pulping the components that keep wood cells together, mainly lignin, are dissolved in order to obtain fibres for papermaking. The aqueous solutions of cooking chemicals are transferred from the lumen through the cell walls towards the middle lamella and the lignin rich middle lamella, which actually binds wood cells together, is dissolved last.[1,3] The most important chemical pulping processes are the kraft and sulphite processes, but due to the better yield and strength properties, the more effective kraft process dominates the sulphite process.

In the sulphite process the cooking liquor is a reaction product of water, sulphur dioxide gas and a base cation (Ca^{2+}, Mg^{2+}, Na^{+}, NH_4^{+}).[1-3] By regulating the composition of cooking liquor sulphite pulping can be carried out in acidic, neutral or alkaline conditions. During sulphite pulping the ether bonds of lignin are hydrolysed and hydrophilic sulphonic acid groups are introduced into lignin. In addition to lignin degradation by hydrolysis, the build up of the phenolic and sulphonic acid groups increases the hydrophilicity of lignin thus improving its solubility.

The strongly alkaline kraft, or sulphate, process is performed in an aqueous solution of sodium hydroxide and sodium sulphide, i.e. in white liquor, at elevated temperatures.[1-3] During kraft pulping lignin fragmentation is also performed by the cleavage of aryl ether bonds and formation of new phenolic groups, which increase the hydrophilicity and solubility of lignin. The reactions of lignin in a kraft cook are complex and still not completely understood, but the main reactions leading to the lignin degradation in alkaline conditions have been well reviewed.[1,2,4-5] The most important delignifying reaction in alkaline conditions is the cleavage of β-aryl ether linkages, which are the most prominent lignin structures. The cleavage of phenolic β-aryl ether bonds is initiated by the formation of quinone methide and elimination of an α-substituent from the phenolate (Fig. 1-1). In kraft pulping conditions the reaction of hydrosulphide ions with quinone methides leads to the cleavage of β-O-4-linkages, whereas in the absence of hydrosulphide ions, such as in the soda cook, the dominating reaction is the elimination of γ-hydroxymethyl or β-proton, which

leads to the formation of formaldehyde and enol ether structures. In addition to hydrosulphide ions, anthraquinone (AQ)[6] and polysulphide (PS)[7] have also been found to enhance the cleavage of β-aryl ether linkages.

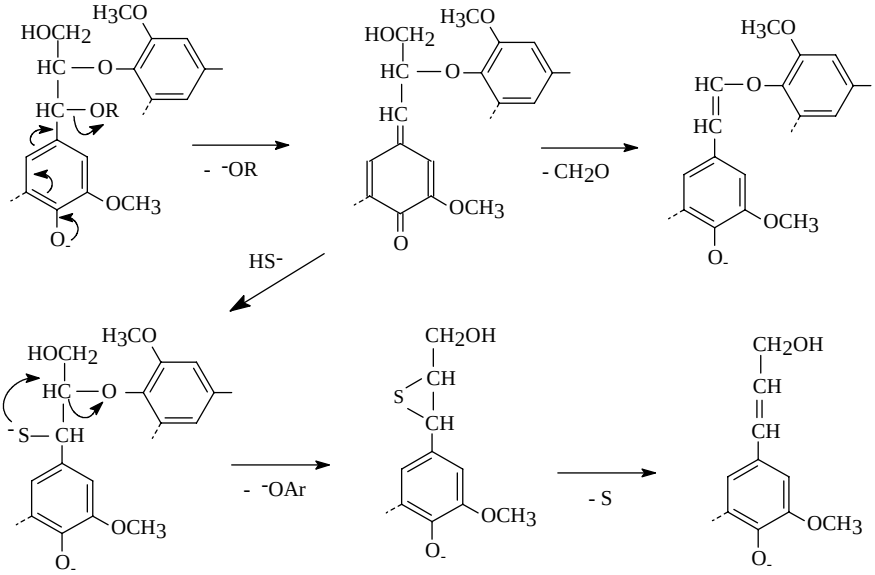

Figure 1-1. *Main reactions of the phenolic β-aryl ether structures in soda and kraft pulping conditions.*[1]

The cleavage of non-phenolic β-aryl ether bonds is the dominating and rate determining reaction in alkaline lignin degradation. The etherified β-aryl ether linkages are cleaved by hydroxide ions via an oxirane intermediate (Fig. 1-2). This reaction is not affected by sodium sulphide or anthraquinone,[4] but for example α-carbonyls have been shown to accelerate the cleavage of β-aryl ether linkages in non-phenolic lignin units.[8,9] Because the reaction is intramolecular, the stereostructure also affects the reactivity and the e*rythro* form of the β-O-4 structure has been found to be more reactive than the corresponding *threo* form.[10-13]

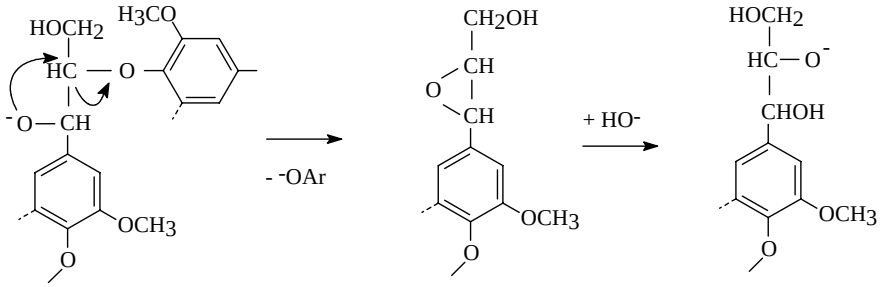

Figure 1-2. *Cleavage of non-phenolic β-aryl ether linkages.*[1]

The phenolic α-aryl ether bonds are cleaved most easily, but since the amount of non-cyclic α-aryl ether structures is low compared to the β-O-4 structures their cleavage does not lead to the major degradation of lignin. The cleavage of the α-ether bonds of phenolic phenyl coumaran structures leads to the formation of alkali stable stilbene structures (Fig. 1-3). The non-phenolic α-aryl ether structures have been reported to be stable.[1,4-5]

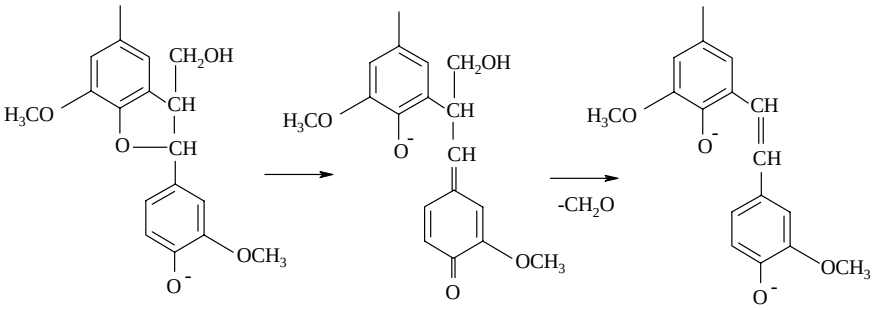

Figure 1-3. *Formation of a stilbene structure from phenyl coumaran in alkali.*[1]

A recently discovered dibenzodioxocin structure, which involves both α- and β-aryl ether bonds within a 8-membered ring, has been reported to be in alkaline pulping conditions less reactive than non-cyclic α-aryl ethers, but more reactive than the ordinary β-O-4 structures.[14,15] During kraft pulping the dibenzodioxocine structures are degraded releasing mainly 5,5'-biphenyl structures (Fig.1-4), whereas in the absence of HS^- ions enol ethers, 5,5'-biphenyls and vanillin are formed.[14]

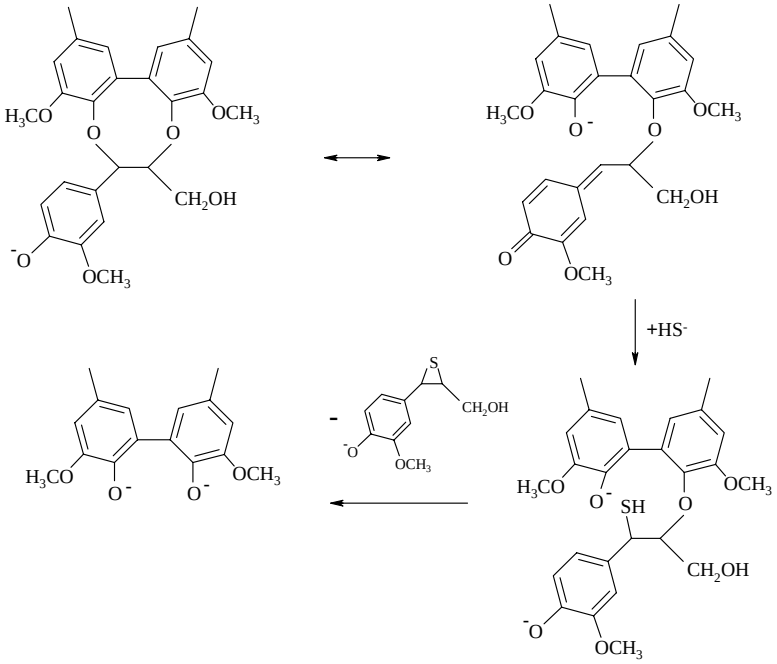

Figure 1-4. *Proposed reaction mechanism for the degradation of dibenzodioxocin structures in kraft pulping conditions.*[15]

In alkaline conditions of pulping, some undesired carbohydrate degradation also takes place.[1,4-5] Owing to the low degree of polymerisation, the amorphous hemicelluloses are more susceptible to degradation and dissolution, but loss of cellulose cannot be avoided either. The end-wise depolymerisation, i.e. peeling, occurs via reducing end groups creating carboxylic acid derivatives. Random alkaline hydrolysis of glycosidic bonds occurs to a lesser extent, but at the same time new end groups are formed and secondary peeling may take place. In modified kraft processes PS and AQ can be used, not only to accelerate delignification, but also to improve the selectivity. Both PS and AQ prevent the peeling of polysaccharides by oxidising their reducing end groups to alkali stable aldonic acids.[16,17]

1.2. Oxygen delignification and bleaching

Towards the end of cooking the selectivity of pulping decreases, preventing the complete removal of residual lignin. In order to avoid severe carbohydrate degradation, further delignification is generally continued by more selective alkaline oxygen delignification. However, only 50% of the residual lignin can usually be removed by oxygen delignification without deterioration of the pulp properties.[3] Especially transition metals are detrimental to oxygen delignification, since they induce the formation of hydroxyl radicals, which facilitate cellulose degradation.[3,5] This reaction can be inhibited by the addition of magnesium salts, which have been shown to reduce the formation of harmful hydroxyradicals.[18]

The reactions involved in alkaline oxygen delignification are complex, including multitude radical chain reactions and the formation of some other oxygen containing species which may contribute to the delignification, e.g. hydroperoxides. According to the proposed reaction mechanism, the phenolic lignin units are converted to phenoxy radicals by the attack of oxygen.[19-21] By further reaction with oxygen the phenoxy radicals are converted into peroxide anions (Fig.1-5), whose intramolecular nucleophilic reaction leads to oxidation of the lignin molecule and formation of muconic acid type carboxylic acid structures as well as oxirane structures, thus increasing the solubility of lignin. Conjugated structures, such as stilbenes and enol ethers formed during pulping are also easily oxidised, leading to fragmentation of lignin by the cleavage of the C_α-C_β bond and the formation of carbonyl structures. Demethoxylation and formation of muconic acids via cathecol intermediates have also been suggested to occur.[22] Condensed 5-5'-biphenyl structures have been shown to be fairly resistant in alkaline oxygen delignification.[23] However, small amounts of the degradation products of 5-5'-biphenyl structures, i.e. 3-carboxy-4-hydroxy-5-methoxy substituted phenolic units, have been found in residual lignin after oxygen delignification.[24]

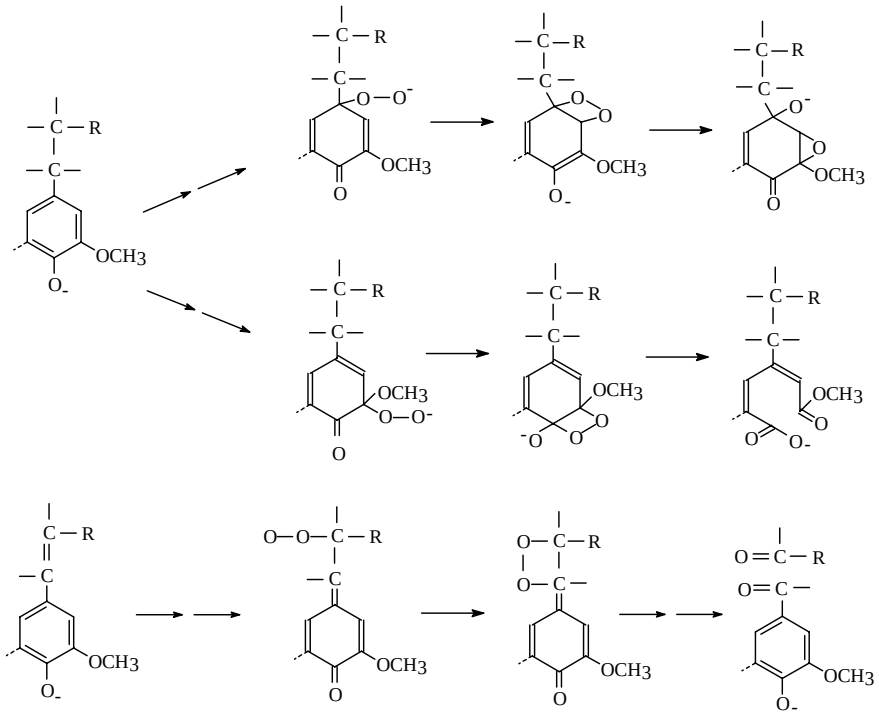

Figure 1-5. *Formation of oxirane, muconic acid and carbonyl structures by intramolecular nucleophilic reaction of peroxide anions in alkaline conditions of oxygen delignification.*[20]

After oxygen delignification, the brightness of the chemical pulp is further improved by lignin-removing bleaching. Nowadays elemental chlorine free (ECF) and totally chlorine free (TCF) bleaching sequences are preferred and typical bleaching agents in addition to oxygen (O) are chlorine dioxide (D), hydrogen peroxide (P), ozone (Z) and sodium hypochlorite (H). Bleaching sequences are combinations of various bleaching steps, involving also alkaline extraction (E), chelation (Q) or some enzyme, mainly xylanase (X), treatments to optimise the removal of residual lignin.[25]

1.3. Proposed obstacles to delignification

The low rate of delignification in the residual phase of pulping has often been suggested to be a consequence of alkali stable lignin-carbohydrate linkages as well as less reactive condensed lignin structures. The location and accessibility of residual lignin may also have a significant effect on the delignification.

1.3.1. Lignin-carbohydrate complexes

Since lignin and carbohydrate components cannot be separated completely by selective chemical treatments or separation methods, a very intimate association between the residual lignin and carbohydrates has been suggested.[26-30] These so called lignin-carbohydrate complexes (LCC) are most likely native,[31-35] but the formation of LC-linkages during pulping has also been shown to be possible.[36-38]

Most of the evidence of covalent LC-bonds is indirect, but lignin and carbohydrates have frequently been proposed to be linked by benzyl ester, benzyl ether and glycosidic linkages.[2,4] Ester linkages are known to be readily hydrolysed in alkali, whereas the α-ether LC-linkages have been shown to be relatively stable under alkaline pulping conditions.[39,40] According to model compound experiments the α-ether LC-linkages, which have been suggested to exist between lignin and all types of wood polysaccharides[31] also retard the cleavage of adjacent β-aryl ether linkages,[40] having thus a negative impact on the delignification. The covalent LC-linkages also increase the extent of cross-linking in lignin molecules and thus decrease the solubility of degraded lignin.[41]

1.3.2. Condensed lignin structures

Condensed aromatic lignin structures have also been suggested to contribute to the incomplete delignification, since the relative amount of mainly C5 substituted guaiacyl structures has been found to increase in residual lignins during kraft pulping[13,42-45] and oxygen delignification.[22,24,43-44,46-47] This may be a consequence of the formation of new condensed structures as well as the enrichment of original condensed lignin structures into fibres due to their less reactive nature.

Condensed 5-5'-biphenyl[42-45] and 5-O-4[42,45] lignin structures have been shown to be less reactive and to accumulate into the fibres during kraft pulping. Recently it was also found that the β-O-4 linkages connected to the condensed structures are more stable under kraft pulping conditions than those connected to non-condensed moieties.[48] However, with model compounds it has been shown that a variety of condensation reactions are possible in

alkaline pulping, leading to the formation of more stable carbon-carbon bonds between lignin units.[1,4-5] New condensed lignin structures, e.g. α-1 and α-5-linkages can be formed by the reactions of quinone methides with carbanions formed in alkaline conditions. Diphenyl methane (DPM) structures have also been suggested to form by the reaction of carbanions with formaldehyde released during pulping by the cleavage of hydroxylated γ-carbon.[49] Formation of DPM structures is more prominent in the absence of HS^- ions, but it has been shown to occur also during kraft pulping.[45] As already mentioned, condensation reactions with carbohydrates are also possible.[36-38]

Especially the C5 substituted DPM[50] and 5-5'-biphenyl[24,44,46-47] structures but also some C6 substituted[43] lignin structures have been shown to be fairly resistant towards oxygen delignification. The corresponding resistance of condensed structures has not been observed towards peroxide or chlorine dioxide.[44,46] Using model compounds it has been shown that the biphenyl structure degrades in oxygen delignification conditions much slower than the corresponding monophenolic structure.[23] This was suggested to be due to the formation of an intramolecular hydrogen bond after ionisation of the other phenolic hydroxyl group, thus making the electron transfer to oxygen more difficult. However, the formation of condensed 5-5'-biphenyl structures by radical coupling reactions during oxygen delignification have also been shown to be possible.[23,47]

1.3.3. Heterogeneous structure and distribution of lignin in softwoods

The accessibility of lignin as well as its reactivity may vary in different morphological regions due to the heterogeneous structure and distribution of lignin within the cell wall and within various constituents of the wood. It is well known that in the middle lamella and the primary wall the concentration of lignin is higher than in the secondary wall, which still contains most of the lignin.[1,2,51] Ray cells and compression wood are also known to be very lignin-rich.[1,51-52] Furthermore, a distinction in the chemical structure of lignin also exists which depends on the origin of the lignin. The content of phenolic lignin units has been reported to be higher in the secondary wall lignin than in the primary wall or middle lamella lignin.[52-53] The molar mass of lignin is also higher in the middle lamella.[54] It has been shown that the etherified lignin units are more condensed than their phenolic counterparts,[55] which is consistent with the results, according to which the lignin structure in the middle lamella is more condensed than in the secondary wall.[54] Also in ray cells lignin has been found to be more condensed and less phenolic than in the other constituents of wood.[52-53] Since the degradation of lignin is mainly driven by the cleavage of aryl ether bonds, whose reaction mechanisms are dependent on whether they are phenolic or non-phenolic, and the condensed lignin structures are supposed to be less reactive, the distribution of those functionalities may have a significant effect on the delignification. It has been shown that in kraft pulping conditions the dissolution rate for lignin in the highly lignified middle lamella and ray cells is lower than that for whole wood.[56]

After kraft pulping, residual lignin is still unevenly distributed and the surface layers of the kraft fibres and the ray cells contain more lignin than the long fibres.[57-59] It has been suggested that two types of LC-complexes exist in the kraft fibres: a high molar mass lignin-galactan complex, which is assumed to originate from the outer layer of the cell wall or compression wood, and a lower molar mass lignin-carbohydrate complex, whose origin is mainly the secondary cell wall.[60-61] The lignin fraction with the higher molar mass was also found to be slightly more condensed than that with the lower molar mass. In addition to the

structural differences, the content of transition metal ions detrimental to oxygen and peroxide bleaching has also been found to be higher in ray cells and on the fibre surface.[58] These factors may greatly affect the uniformity of further delignification. It has been reported that kraft pulp without ray cells consumed considerably less active chlorine in order to obtain a certain brightness level than the original pulp.[62] Higher viscosity and lower peroxide consumption have been reported for a pulp, which was peeled before TCF-bleaching in order to remove lignin rich ray cells and fibre surface material.[58] The lower content of transition metals after removal of surface material also results in the reduced degradation of peroxides and formation of detrimental hydroxyl radicals which induce cellulose degradation.[58]

1.4. Objectives of the study

In this thesis, modern NMR spectroscopic techniques were applied to investigate the changes occurring in the structure of polymeric wood components during various chemical pulping related processes. Due to its non-destructive nature and versatility, NMR spectroscopy is a very valuable method in studies of lignocellulosics. By solid-state NMR methods the components of wood and pulp can be analysed *in situ* and investigations of the morphology of cellulose as well as the suggested interactions between lignin and carbohydrates are possible. Poorly soluble residual lignin-carbohydrate complexes (RLCC) can also be analysed reliably and no distinction is made between phenolic and non-phenolic lignin units. Due to the better resolution, multidimensional NMR methods in solution can be utilised for more detailed structural analysis of lignin side-chain structures.

Since cellulose morphology may have an effect on the strength properties of pulp, but also give information on the accessibility and degradation mechanisms of cellulose during pulping and bleaching, the high-resolution solid-state NMR spectroscopic techniques were used in this thesis to investigate the morphology of cellulose after various pulping processes as well as after oxygen delignification and TCF-bleaching. The degree of cellulose crystallinity and the relative proportions of cellulose polymorphs were determined.

In order to learn to understand better the lignin reactions, solid-state NMR spectroscopy and multidimensional liquid NMR methods were utilised to monitor the effects of kraft pulping and oxygen delignification on the structure of softwood lignin. Due to the suggested unreactivity of condensed lignin structures, the extent of condensation in various technical lignins was studied in solid state by a dipolar dephasing technique. For the same reason, the interactions between lignin and carbohydrates in RLCC were also investigated by proton spin-lattice relaxation and HETCOR measurements in the solid state.

One of the main objectives of this research was to investigate if some parts of the fibre are unequally affected by kraft pulping. Therefore the structure of residual lignin and the crystallinity of cellulose in ray cells and on the fibre surface were compared with the corresponding structures inside the fibre by isolating fines fractions before and after refining of kraft pulp. In addition to the cellulose crystallinity, the lateral dimensions of cellulose fibrils and fibril aggregates were determined.

All the pulp and lignin samples studied in this thesis were produced at the Finnish Pulp and Paper Research Centre, KCL.

2. NMR SPECTROSCOPIC TECHNIQUES USED

2.1. High-resolution solid-state NMR spectroscopy in cellulose and lignin studies

Due to its capability of measuring samples in their native state, ^{13}C Cross-Polarization Magic Angle Spinning (CPMAS) NMR spectroscopy can be applied to investigate both the chemical and physical structure of lignocellulosics. Therefore in addition to the chemical structure of lignin, ^{13}C CPMAS was used in this thesis also to investigate the morphology of cellulose and the interactions of lignin and carbohydrates within the cell wall.

2.1.1. ^{13}C CPMAS NMR spectroscopy in morphological studies of cellulose

It is characteristic of NMR spectra that chemically equivalent carbons can be distinguished if they are magnetically non-equivalent. So even though the corresponding carbons of different anhydroglucose units of cellulose are chemically equivalent, they can be distinguished in a ^{13}C CPMAS spectrum if they are in different magnetic environments, for example due to the different packing of the cellulose chains or distinct conformations. Separate signals for amorphous and crystalline carbons as well as splitting of crystalline signals due to cellulose polymorphs can thus be detected.

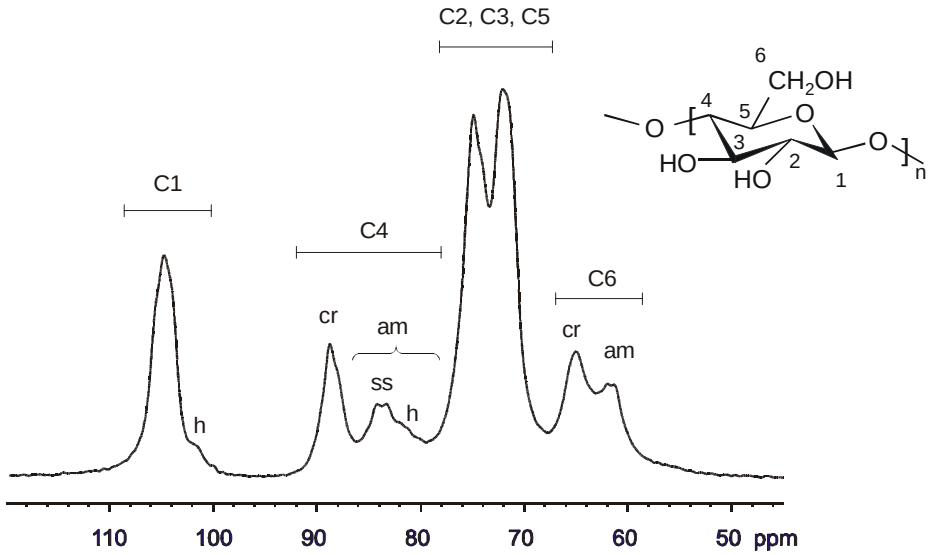

Figure 2-1. *^{13}C CPMAS spectrum of spruce kraft pulp. Cr=crystalline, am=amorphous, s=crystallite surfaces and h=hemicelluloses.*

The ^{13}C CPMAS spectrum of spruce kraft pulp is shown in Figure 2-1. The most informative region in the cellulose spectrum is the C4 region between 79 and 92 ppm. The sharper signal at 86-92 ppm corresponds to the highly ordered cellulose of the crystallite interiors, whereas the broader upfield signal (79-86 ppm) has been assigned to the disordered cellulose as well as to the less ordered cellulose chains of the crystallite surfaces.[63-68] Cellulose of the crystallite surfaces has been shown to give the doublet at 83.5 and 84.5 ppm.[69-71] Recently, based on solvent-exchange, spin-relaxation and spin-diffusion experiments, this doublet has

been reported to indicate the accessible fibril surface, whereas the broader signal assigned earlier to the amorphous cellulose, has been reported to indicate inaccessible fibril surfaces.[72-74] Cellulose spectra have been shown to be quantitative within a few percent accuracy for both dry and wet samples,[69,75-77] but in order to obtain quantitative spectra of pulp cellulose, the samples must be free of lignin and hemicelluloses.[77]

2.1.1.1. Determination of cellulose crystallinity

Only the highly ordered cellulose in the interiors of the crystallites is considered in this thesis as 'crystalline' cellulose. The term 'amorphous' is correspondingly used to describe the remaining less ordered cellulose, thus also including the fibril surfaces. The degree of crystallinity in various pulp samples was determined as a crystallinity index (CrI) from the areas of the crystalline and amorphous C4 signals by deconvolution using a Lorenzian line shape.[67,75,78, I-III]

$$CrI = A_{86\text{-}92ppm} / (A_{79\text{-}86ppm} + A_{86\text{-}92ppm}) \cdot 100\% \qquad (2.1)$$

Results obtained by this method for pure cellulose samples have been shown to well correlate with the corresponding results obtained by X-ray diffraction.[67,75] However, in pulp and wood samples, hemicelluloses and lignin side-chains also contribute to the area of the 'amorphous region'.[72-73,79-81] Therefore, the interfering hemicellulose and lignin signals must be removed either chemically[72,77] or spectroscopically[78,82-84] before the determination of CrI. The utilisation of chemometric methods has also been reported.[85]

2.1.1.2. Spectral edition based on proton spin-relaxation

The proton spin-relaxation based spectral edition (PSRE) method has been frequently used to investigate the cellulose crystallinity in wood[78,82-83] and pulp.[84] In the PSRE-method the differences in the proton spin-relaxation times ($T_{1\rho H}$) of different spatial domains are utilised to separate the components into subspectra of their own. In this way, the interference of lignin and hemicellulose signals resonating in the amorphous region can be removed spectroscopically and all the possible structural changes affected by chemical treatments are avoided.

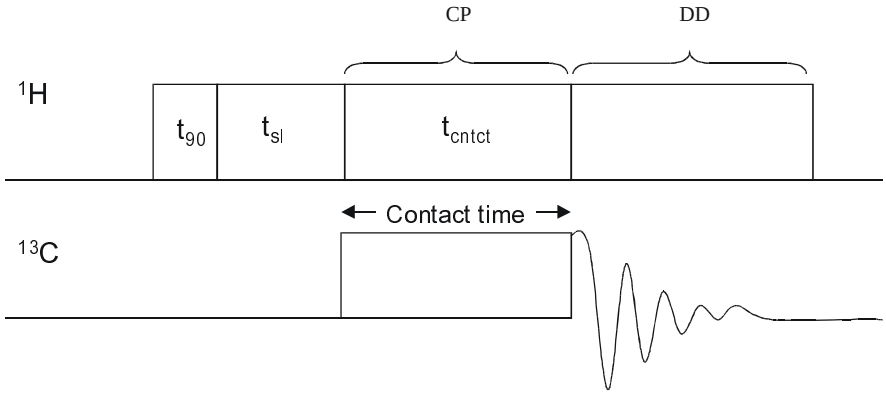

Figure 2-2. *Delayed contact pulse sequence.*[78]

The 'delayed contact' pulse sequence (Fig. 2-2) used in the PSRE-method[78] was also applied in this thesis to separate the subspectra of cellulosic and non-cellulosic components.[III] In addition to the ordinary cross-polarization, this pulse sequence has a spin-lock delay (t_{sl}) between proton preparation pulse (t_{90}) and contact time (t_{cntct}). During the spin-lock t_{sl}, some loss of the magnetization occurs through relaxation, which is faster for the amorphous lignin and hemicellulose matrix than for the more ordered cellulose component. Based on different relaxation times due to the different mobilities, the subspectra of crystalline cellulose and the amorphous matrix can be separated (Fig. 2-3). Since the relaxation times of the domains are quite similar in magnitude, a linear combination of two spectra measured with different spin-lock times is required to obtain subspectra of the components. Relaxation times of lignin and hemicelluloses have been observed to be indistinguishable and therefore those components are inseparable.[78] To find an appropriate linear combination of the spectra measured with different t_{sl}, the procedure described by Newman *et al.* [70,86]and Lopez *et al.*[87] was followed.

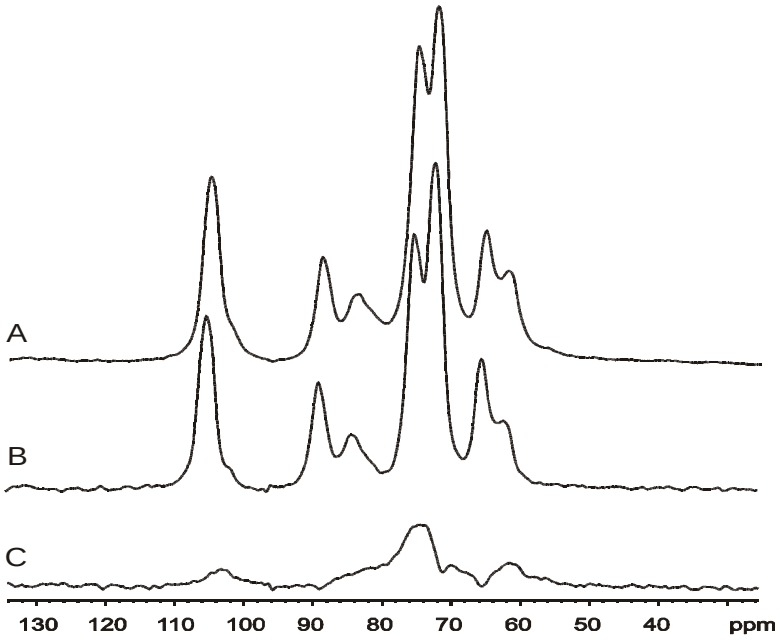

Figure 2-3. *a) ^{13}C CPMAS spectrum of kraft pulp and the subspectra of b) more ordered cellulose and c) amorphous components. Spectra measured with t_{sl}=0ms (S) and t_{sl}=8ms (S') were used for linear combinations. Crystalline component: 0.74S+2.77S', amorphous component: 1.74S-2.77S'.*

2.1.1.3. Determination of cellulose polymorphs

Crystalline cellulose exhibits various polymorphs, of which the natively synthesised cellulose I is most common. Based on results from ^{13}C CPMAS NMR spectroscopy, VanderHart and Atalla discovered that the crystalline region of native cellulose I is a mixture of two crystalline forms, cellulose I_α and I_β, and their relative proportions vary depending on the species.[68] Cellulose I_α is the dominant form in bacterial and algal celluloses, whereas cellulose I_β is the dominant form in higher plants, such as cotton and tunicate celluloses.[68,88] In softwoods the proportion of cellulose I_α has also been reported to be higher than in hardwoods.[82] It has been shown that cellulose I_α has a one-chain triclinic unit cell whereas cellulose I_β has a two-chain monoclinic unit cell.[89] A difference in their hydrogen-bonding pattern has also been suggested.[90] By annealing, the metastable cellulose I_α can be converted to the more stable I_β form,[91-92] and by mercerisation or by regeneration from a solution,

cellulose I can be transformed to cellulose II. Small amounts of cellulose II have also been detected in pulps[93] and in samples commonly thought to contain only cellulose I, such as cotton[93] or bacterial cellulose.[94-95] The other cellulose polymorphs, III and IV, are not considered in this thesis.

The occurrence of various crystalline forms of cellulose can be observed in the ^{13}C CPMAS spectrum as a splitting of the crystalline signals. The splitting is most prominent in the crystalline C4 signal, which was used also in this thesis to determine the relative proportions of cellulose polymorphs by using the signal areas determined by deconvolution.[I-III] The assignment of the cellulose polymorphs was made using highly crystalline samples, rich in either cellulose I_α (*acetobacter xylinum*), cellulose I_β (cotton linter) or cellulose II (mercerised cellulose),[I] shown in Figure 2-4.

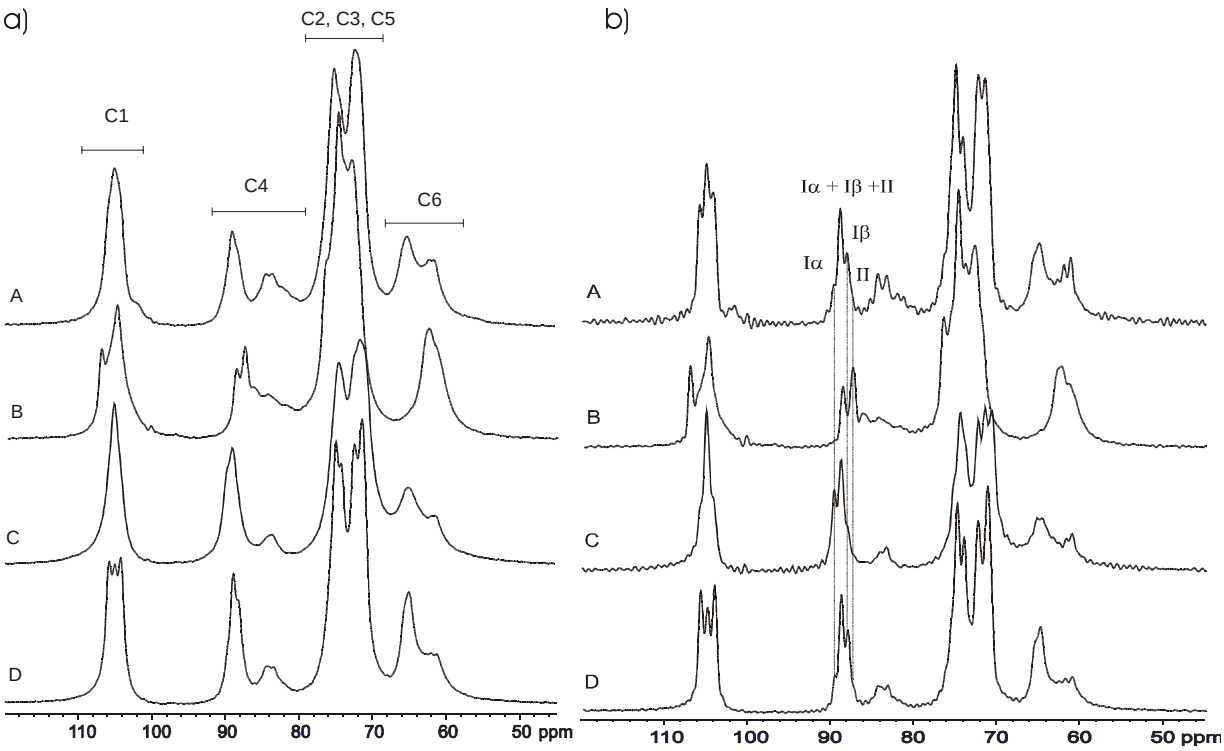

Figure 2-4. *a) Ordinary ^{13}C CPMAS spectra of kraft pulp (A), mercerised kraft pulp (B), Acetobacter xylinum (C) and cotton linter (D). b) The same spectra after resolution enhancement.*

In the ^{13}C CPMAS spectra of wood and pulp the resolution is low, thus preventing the observation of different polymorphs. The resolution can, however, be improved by a mathematical method, i.e. 'resolution enhancement' in which FID is multiplied by the function $f(t)=\exp\{at^n-bt^m\}$,[96] where n=1-2 and m=2-3.[82,91] This is a commonly used method in solution NMR spectroscopy, but due to the transformation of the lineshape from Lorenzian into Gaussian during the procedure, it is not an ideal method for solid-state NMR spectra in which the lineshape is rather Gaussian than Lorenzian.[96] Resolution enhancement is, however, quite commonly used in the ^{13}C CPMAS studies of cellulose polymorphs[82,91,97-99] and it was used also in this thesis before the deconvolution of crystalline C4 signal, in order to determine the relative proportions of cellulose polymorphs.[I-III] By spectral simulation, it has been shown that the splitting caused by the resolution enhancement into

crystalline signals is not an artefact.[99] The increased noise level involved with this method, however, exposes the deconvolution of small signals to errors and, therefore, the determination of the proportion of cellulose II is not very accurate. To avoid resolution enhancement, principal component analysis has also been utilised by some researchers to determine the relative proportions of cellulose polymorphs in pulp.[100-101]

2.1.1.4. Determination of the lateral dimensions of cellulose fibrils and fibril aggregates

In the fibre cell wall, cellulose chains are considered to form fibrils, which may be further associated to form larger fibril aggregates. Due to the difference in chemical shifts of the crystallite interiors and the crystallite surfaces, solid-state NMR spectroscopy can be applied to determine the average lateral fibril dimension (LFD) from the quantitative ^{13}C CPMAS spectra of pure cellulose.[72,86,102-103] The difference in the chemical shifts of accessible and inaccessible fibre surfaces also allows the determination of lateral fibril aggregate dimensions (LFAD).[77,104]

The spectral fitting method developed in the Swedish Pulp and Paper Research Institute (STFI)[69,72] was used in this thesis to determine the average lateral dimensions of fibrils and fibril aggregates.[IV] This method is based on the model of aggregated cellulose fibrils, suggested by Wickholm (Fig. 2-5).[74] The spectral fitting showing the corresponding chemical shifts for C4 region is presented in Figure 2-6.

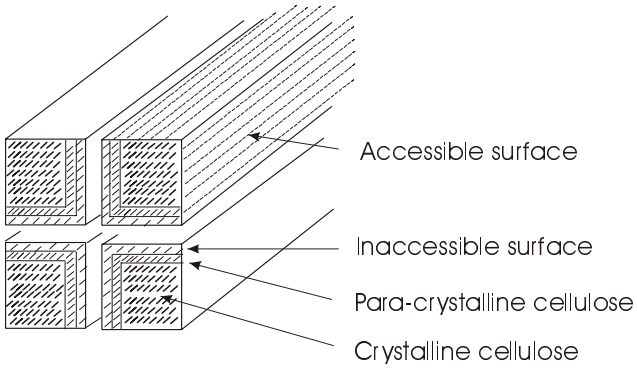

Figure 2-5. *Schematic model of four aggregated cellulose fibrils according to Wickholm.[74]*

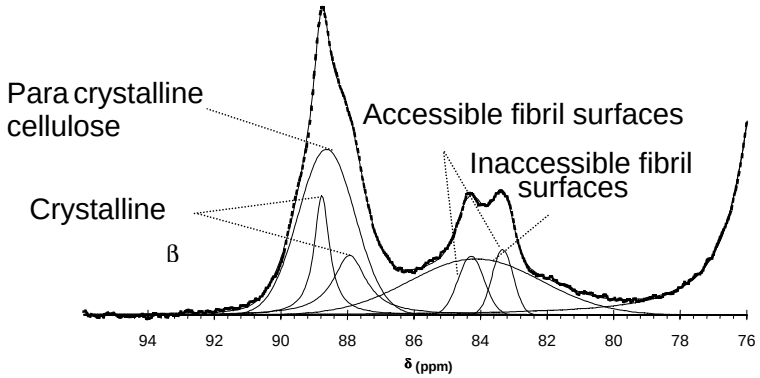

Figure 2-6. *Spectral fitting for the C4 region of the kraft fibre fraction isolated after sequential refining of kraft pulp.* [IV]

According to the model, cellulose fibrils and fibril aggregates are assumed to have square cross sections. The average lateral fibril dimension can thus be determined according to equation (2.2), where the fraction (q) is the signal intensity of both accessible and inaccessible surfaces in relation to the total intensity of the C4 signal area. The fibril aggregate dimension can be resolved similarly using the fraction of the signal intensity from the accessible surfaces.

$$q = (4n-4)/n^2 \qquad (2.2)$$

In equation (2.2), n is the number of cellulose polymers along one side of the assumed square fibril or fibril aggregate cross-section. An average distance of 0.57 nm per cellulose chain has been used to determine the fibril size.[86,89] Before the measurements, hemicelluloses and lignin were removed from the pulp samples by chlorite delignification and acid hydrolysis in order to obtain quantitative CPMAS spectra for cellulose.[72,77,104, IV]

2.1.2. High-resolution solid-state NMR spectroscopy in structural studies of lignin

Solid-state ^{13}C CPMAS spectroscopy provides a very valuable tool also for lignin studies. It can be very well utilised for example in studies of enzymatically isolated residual lignin-carbohydrate complexes (RLCC), which have restricted solubility. In this way the whole lignin sample can be analysed reliably and not just some soluble fraction of it. No chemical modifications for the sample preparation, such as acetylation that is often used in solution NMR to improve the solubility, are needed. In addition, both free phenolic and etherified lignin units can be equally investigated. The major drawback of CPMAS spectroscopy is, however, its low resolution compared to the solution state NMR spectroscopy, and therefore only some structural features of lignin can be investigated instead of detailed structures. A characteristic ^{13}C CPMAS spectrum of softwood residual lignin is shown with its assignments in Figure 2-7.[105-107] The low resolution can, however, be compensated by many special techniques, which allow for example the determination of the degree of condensation in lignin or the investigation of interactions between lignin and other wood components.

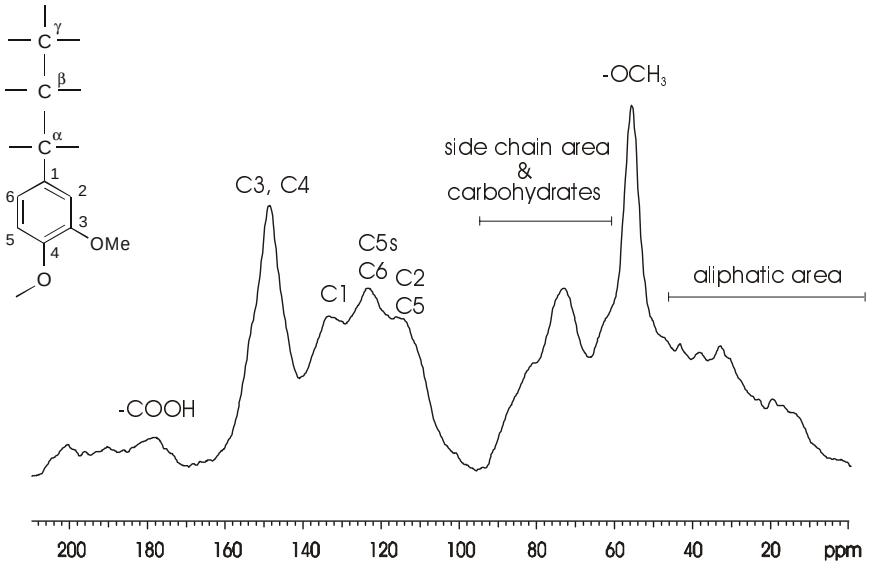

Figure 2-7. *^{13}C CPMAS spectrum of a residual lignin of kraft pulp. C5s= substituted C5.*

2.1.2.1. Dipolar dephasing technique

The 'dipolar dephasing' technique[108] can be applied to estimate the extent of condensation, i.e. the average extent of substitution of the aromatic rings of lignin. In this technique, the dipolar interactions between protons and carbons are utilised to cause the dephasing of the signals by turning off the high-power decoupler for a short while (d2) between the cross-polarization and the data acquisition (Fig. 2-8). During the d2-delay, the dipolar interactions between protons and carbons induce a fast dephasing of the signal, which is most rapid with the protonated carbons due to the close proximity of attached protons.

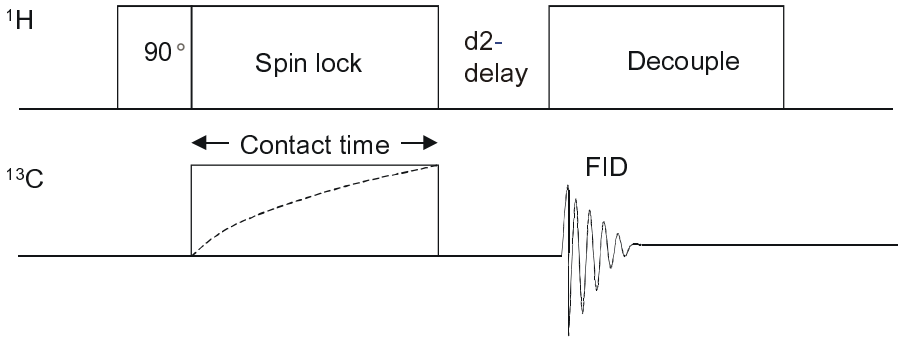

Fig. 2-8. *The dipolar dephasing pulse sequence.*[108]

A/B-method

By selecting a suitable delay, during which the dipolar interactions are allowed to take effect it is possible to detect only quaternary carbons due to the faster decay of the protonated carbon signals.[109-110,III,V-VI] The ordinary ^{13}C CPMAS spectrum measured without any delay, and the dipolar dephasing spectrum measured with the 50 μs d2-delay, are shown in Figure 2-9 for a residual lignin sample. The signal A (~140-160 ppm) in dipolar dephasing spectrum is due to the C3 and C4 of the guaiacyl group, whereas the signal B (~115-140 ppm) is due to the C1 and the substituted C5 of the guaiacyl group. Therefore, the ratio of these signal areas (A/B) provides information on the extent of aromatic substitution and the degree of condensation. The lower the ratio A/B, the higher is the degree of condensation. Similarly, this method has been utilised to determine the ratio of the syringyl and guaiacyl units in hardwood lignin.[109-110]

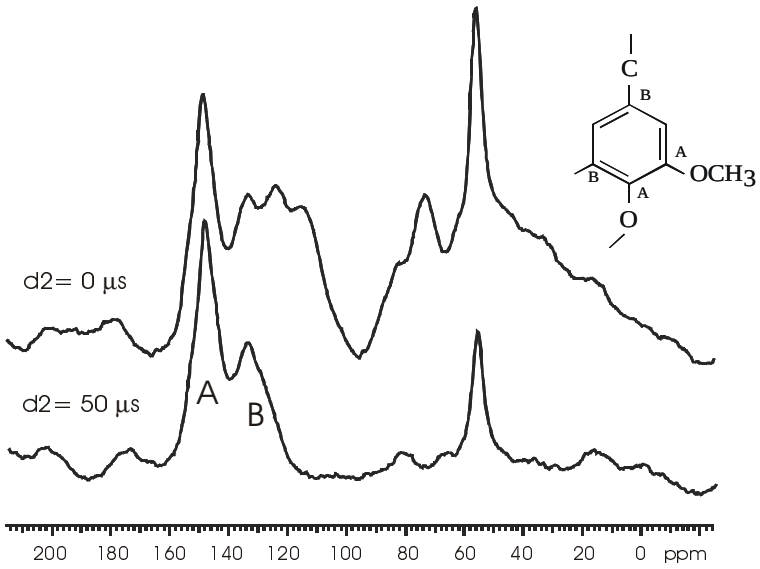

Figure 2-9. *The ^{13}C CPMAS (d2=0 µs) and the dipolar dephasing (d2=50 µs) spectra of a residual lignin of kraft pulp.*

D2-array method

The average extent of substitution of the aromatic ring can also be determined by monitoring the unequal decay rates of the protonated and quaternary carbon signals.[VI] This method has previously been applied to determine the extent of condensation in lignin of various naturally degraded and fossilised soil and coal samples.[111-113]

In this d2-array method the natural logarithm of the area of the aromatic region (~100–160 ppm) is observed as a function of the d2-delay time (Fig. 2-10). The total intensity (I_{tot}) of the aromatic region is composed of the intensities of the faster decaying protonated carbons (I_a) and the slower decaying quaternary carbons (I_b). The decay of the total intensity can be described by the equation (2.3), in which T'_{2a} and T'_{2b} are decay constants and T_{d2} is the delay time d2. [114]

$$I_{tot} = I_a + I_b = I_a^0 e^{-T_{d2}^2 / T_{2a}^{'2}} + I_b^0 e^{-T_{d2} / T_{2b}^{'}} \qquad (2.3)$$

The decay of the signal intensity, when d2 ≥ 50 µs is linear and describes only the decay of the non-protonated carbons (Fig. 2-10b). By fitting a straight line to this data, the initial intensity I_b^0 of the quaternary carbons at d2=0 can be obtained from the intersection of the y-axis, and the constant T'_{2b} from the slope of the fit. With the aid of these values the intensity contribution of the quaternary carbons can be subtracted from the total intensity and I_a^0 at d2=0 can be resolved similarly by fitting a curve to this data. The fraction of the protonated aromatic carbons (f^H) and the number of the protonated carbons (CH_{number}) in the guaiacyl ring can then be resolved using equations (2.4) and (2.5).[111-113]

$$f^H = I_a^0/(I_a^0+I_b^0) \qquad (2.4)$$

$$CH_{number} = 6f^H \qquad (2.5)$$

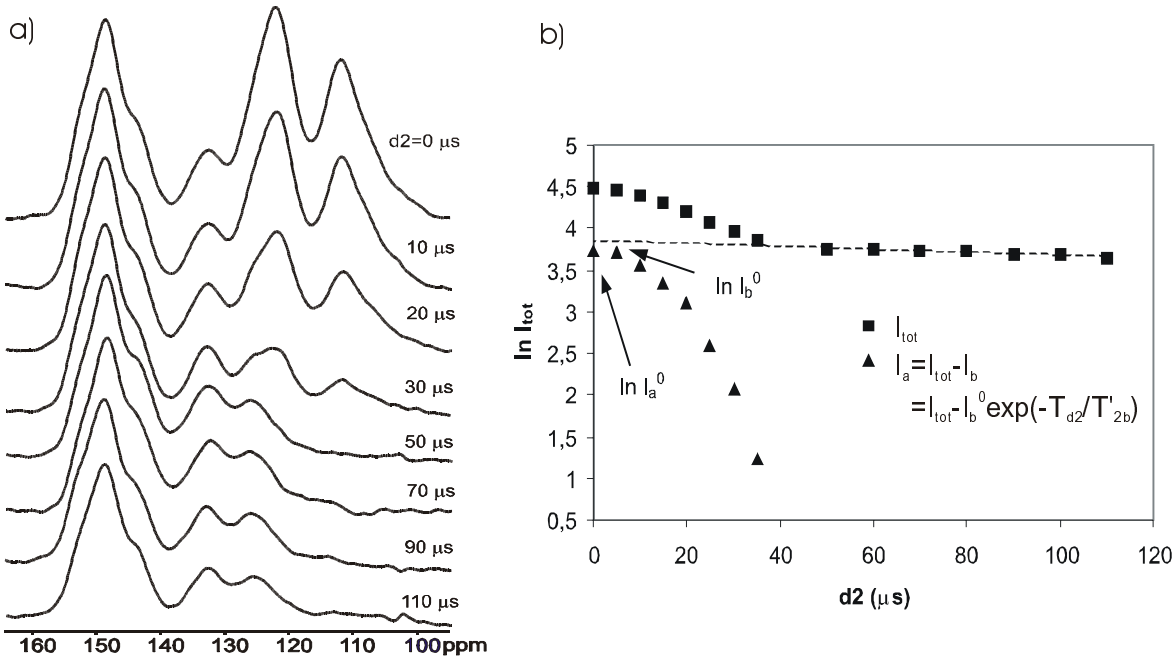

Figure 2-10. *a) The aromatic region of the dipolar dephasing spectra of 5-5'-biguaiacylglyserol-β-guaiacyl ether model compound with various d2-delays. b) Decay of the ln I_{tot} as a function of d2-delay for the same model compound.*

With model compound experiments it has been shown that both methods can be applied to determine the extent of condensation in lignin.[VI] However, the d2-array method was found slightly more reliable than the A/B-method, although carbohydrates and all other impurities resonating at the aromatic region have an interfering effect.

2.1.2.2. Interactions between lignin and carbohydrates

In cellulose studies, the different relaxation behaviours of various wood components can be used to separate cellulose and non-cellulosic matrix into subspectra, but proton spin-lattice relaxation times (T_{1H}, $T_{1\rho H}$) can also be utilised to monitor the homogeneity of the sample and the association of the components.[115] Due to the suggested LC-complexes especially the interactions of lignin and carbohydrates have been a matter of great interest.[33,116-119] Equal proton spin-lattice relaxation times (T_{1H}) of different components indicate intimate contact at the molecular level and homogeneity at domains of some tens of nanometres, whereas equal proton relaxation times in the rotating frame ($T_{1\rho H}$) provide information on the homogeneity on the scale of a few nanometres.[120]

In two-dimensional solid-state ^{13}C-^{1}H heterocorrelation (HETCOR) experiments the correlations of carbons and protons are observed not only through the covalent bonds but also through space.[121] Therefore, also HETCOR experiments can be utilised to investigate the homogeneity as well as the chemical interactions between components, as it has been shown with synthetic copolymers[122] and polymer blends.[123] In this thesis, HETCOR experiments were used to investigate the interactions between lignin and carbohydrates.

2.2. Modern multidimensional solution NMR techniques in lignin characterization

In solution, a much better resolution is obtained than in solid-state and a more detailed characterization of the lignin side-chain structure is possible. In traditional one-dimensional ^{1}H and ^{13}C NMR spectra the signals heavily overlap due to the very complex and heterogeneous structure of lignin. However, modern two- and three-dimensional techniques have proved to be efficient in investigations of lignins.[124-126] Besides a better resolution, the multidimensional techniques also bring more reliability to the assignments of lignin structures. The utilisation of solution NMR in lignin studies has recently been reviewed by Ralph *et al*.[127] In this thesis, 2D HSQC and 3D HSQC-TOCSY techniques were applied to investigate the lignin side-chain structure.[VII]

Two-dimensional ^{1}H-^{1}H Total Correlation Spectroscopy (TOCSY) enables the detection of through-bond connectivities between protons.[128] Depending on the spin-lock time used in the measurement, it is possible to see the ^{1}H-^{1}H couplings of protons throughout the whole spin system and thus, it is possibile to identify the correlations that belong to the same spin system. In the case of lignin, each phenyl propane side-chain forms a spin system, which can be utilised to identify various bonding patterns. Two-dimensional ^{1}H-^{13}C Heteronuclear Single Quantum Correlation Spectroscopy (HSQC) measurements reveal the connectivities between protons and directly bonded carbons.[128] However, the overlapping of the lignin signals cannot be fully avoided even by these 2D experiments and the spectra are still very crowded with signals.

In the three-dimensional HSQC-TOCSY method,[129] both TOCSY and HSQC techniques are combined to build up a 3D experiment. In addition to the improved resolution, the 3D HSQC-TOCSY spectra provide more reliability to the assignments of the lignin structures, as the connectivities can be cross-checked from the different planes of the 3D spectrum. The HSQC planes give through bond connectivities of protons and carbons, while the TOCSY planes connect these to the other protons of the ^{1}H-^{1}H spin-system. The 3D HSQC-TOCSY spectra can thus be utilised to connect individual correlations in the 2D HSQC spectra together to form complete lignin side-chain spin-systems. Contrary to using only 1D or 2D data, this approach is independent of the model compound data, as no prior knowledge of the connectivities is needed to collect the ^{1}H- and ^{13}C- chemical shifts together. Therefore, the assignments do not rely on the chemical shifts only, but also on the connectivities between them, and the whole ^{1}H- and ^{13}C-spin-system can be used to identify individual lignin side-chain linkages. The utilisation of 3D NMR spectra in the interpretation of lignin assignments has been described in more detail elsewhere.[124-126]

3. RESULTS AND DISCUSSION

3.1. Cellulose crystallinity

3.1.1. Effects of kraft and sulphite pulping

(Papers I, II & some unpublished data)

The solid-state NMR spectroscopic methods described in section 2.1.1 were applied to investigate the effects of kraft and sulphite pulping on the crystallinity of cellulose in spruce wood.[I,II] The results presented in Table 3-1 show clearly that the CrI_{CPMAS} values obtained by the ordinary ^{13}C CPMAS measurements for spruce wood (27%) and pulps (45-50%) are very sensitive to the variations of the lignin and hemicellulose contents. Therefore, in order to obtain quantitative cellulose spectra, amorphous lignin and hemicelluloses were removed by the proton spin-relaxation based spectral edition (PSRE) method before the determination of cellulose crystallinity (CrI_{PSRE}).

Table 3-1. *The crystallinity indices determined by the ordinary ^{13}C CPMAS (CrI_{CPMAS}) and PSRE (CrI_{PSRE}) methods, together with the relative proportions of cellulose polymorphs.*

	Lignin content (%)	**Glucose content (%)[1]**	**CrI_{CPMAS} (%)**	**CrI_{PSRE} (%)**	**Iα (%)**	**Iβ (%)**	**II (%)**
Spruce wood	27.2	66.7	27 [2]	58 (2)[3]	74	26	-
Kraft pulp (unbleached)	4.8	83.5	50	68 (3)	26	64	10
Kraft pulp (ECF)[4]	-	82.2	47	72 (1)	30	61	9
Sulphite pulp (ECF)[4]	-	80.6	45	71 (2)	39	49	12

[1]Glucose content in relation to other monosaccharides. [2] An errorneous CrI value was given in Paper I, Table 1 for spruce. [3] Standard deviation. [4] ODEDED-bleaching sequence (O=oxygen, D=ClO_2, E=NaOH extraction).

According to the CrI_{PSRE} results, the degree of cellulose crystallinity increases during pulping. The increase in crystallinity is most likely due to the preferential loss of less-ordered cellulose,[84,130-131] but some further ordering of cellulose may also take place,[77] as will be discussed below. No difference in cellulose crystallinity between the kraft and sulphite pulps was observed. The ECF-bleaching may have a slight increasing effect on crystallinity, but the exact effect of the ECF-bleaching on crystallinity was not investigated in this thesis.

The relative proportions of cellulose polymorphs show that cellulose I_α predominates over cellulose I_β in spruce wood. During kraft and sulphite pulping, some of the metastable cellulose I_α is converted to the more stable I_β form. This is mainly induced by the high temperature used in pulping (170°C in kraft pulping), but the alkaline cooking liquor has also been shown to accelerate the transformation.[91,132] In sulphite pulp the relative proportion of cellulose I_α is still clearly higher than in the kraft pulp samples studied. This is most likely due to the lower temperature (140°C) used in sulphite cooking conditions,[101] but the composition of the cooking liquor may also have an effect. In addition to the conversion of cellulose I_α to I_β, it is possible that some unordered cellulose has been recrystallized as cellulose I_β, or cellulose I_β is more resistant to degradation. It has recently been shown that

during kraft pulping the lattice distortions in the interior of the cellulose crystallites are converted to cellulose I_β,[77] thus also having an increasing effect on the crystalliny of cellulose.

A small amount of cellulose II was found in kraft and sulphite pulps, as also reported earlier.[93,101] However, due to the insufficient resolution of the cellulose II signal, it cannot be concluded if this cellulose fraction is native or formed during kraft pulping.

3.1.2. Pine and birch pulps with various hemicellulose contents

(Unpublished data)

ECF-bleached pine and birch pulps containing varying amounts of hemicelluloses were compared in order to investigate the effects of various pulping methods and hemicellulose contents on the crystallinity of cellulose.[133] Polysulphide pulping with anthraquinone (PS-AQ) is known to be a hemicellulose preserving pulping method, whereas flow-through kraft pulp (FT-Kraft) usually contains less hemicelluloses than conventional kraft pulp (Kraft). In addition to the CrI_{CPMAS} values obtained by ordinary ^{13}C CPMAS measurements, the degree of cellulose crystallinity was determined after removing hemicelluloses spectroscopically (CrI_{PSRE}) or chemically by acid hydrolysis ($CrI_{CPMAS+AH}$), in order to compare the methods. The acid hydrolysis was conducted in 2.5M HCl at 100°C for 4 or 17h. The results obtained are presented in Table 3-2.

Table 3-2. *Cellulose crystallinities determined before (CrI_{CPMAS}) and after 4h or 17h acid hydrolysis ($CrI_{CPMAS+AH}$) by ordinary ^{13}C CPMAS as well as by the PSRE method (CrI_{PSRE}) for ECF-bleached[1] pine and birch pulps.*

	Glucose content[2] (%)			**CrI_{CPMAS} (%)**	**CrI_{PSRE} (%)**	**$CrI_{CPMAS+AH}$ (%)**	
Pine:	**Before AH[3]**	**4h AH**	**17h AH**			**4h AH**	**17 h AH**
FT-Kraft pulp	88.2	-	97.0	56	70 (1)[4]	61	65
Kraft pulp	84.3	92.6	97.4	52	71 (3)	61	63
PS-AQ pulp	81.7	-	96.7	49	68 (4)	57	62
Birch:							
FT-Kraft pulp	78.0	-	98.5	43	53 (2)	-	60
Kraft pulp	75.4	95.1	98.6	41	56 (3)	56	59
PS-AQ pulp	73.3	-	98.9	39	51 (2)	-	60

[1] OD(EO)D_ND-sequence (O=oxygen, D=ClO_2, E=NaOH extraction). [2] Glucose content in relation to other monosaccharides. [3] AH = acid hydrolysis. [4] Standard deviation in parenthesis

3.1.2.1. Comparison between chemical and spectroscopic removal of hemicellulose signals

According to Table 3-2, the lower CrI_{CPMAS} values correlate again with the higher hemicellulose contents of the pulps. This can be seen clearly between pine and birch pulps as well as between FT-Kraft, Kraft and PS-AQ pulps. After removal of hemicelluloses, higher CrI values are obtained. However, the numerical values obtained by CrI_{PSRE} and $CrI_{CPMAS+AH}$

methods differ significantly and are thus not directly comparable. The trends between studied samples are similar for both methods.

The crystallinities obtained for pine samples after acid hydrolysis ($CrI_{CPMAS+AH}$) are lower than the corresponding crystallinities obtained by the PSRE-method (CrI_{PSRE}). For birch samples just the opposite was observed, as will be discussed in more detail in section 3.1.2.2. The lower $CrI_{CPMAS+AH}$ values of pine pulps are at least partly due to the incomplete removal of hemicelluloses by acid hydrolysis. After 4h acid hydrolysis the glucose contents in pine and birch pulps are 93 and 95%, respectively, and even after 17h hydrolysis the glucose contents are 97 and 99%, respectively (Table 3-2). This variation in glucose contents can be seen directly in the $CrI_{CPMAS+AH}$ values, which are very sensitive even to slight differences in the amounts of hemicelluloses.

Another drawback of acid hydrolysis is the dissolution of cellulose during the treatment (Table 3-3). It is generally accepted that the crystalline regions are more resistant to hydrolysis, while the amorphous cellulose is more readily dissolved by dilute acids. In similar conditions as used in this work, it has been shown that in the early stage of the hydrolysis some further crystallisation occurs, but after reaching the levelling off degree of polymerisation, i.e. after 15 min exposure, the disordering of crystalline cellulose takes place.[134] In highly acidic conditions the crystallinity of cellulose was found to decrease dramatically even after very short times of exposure.[I] However, during acid hydrolysis the original equilibrium state between crystalline and amorphous cellulose is changed and the exact effect of the acid hydrolysis on the cellulose crystallinity of pulp is not known.

By using the purely spectroscopic PSRE-method, all the possible structural changes due to the chemical treatments can be avoided and the pulp cellulose can be analysed *in situ*. The higher CrI_{PSRE} values obtained for the pine pulps also indicate that the amorphous non-cellulosic components can be removed more effectively by the PSRE method than by acid hydrolysis. It is therefore concluded that the PSRE-method is a more convenient way to remove the interfering hemicellulose signals from softwood pulps.

Table 3-3. *The monosaccharide composition of carbohydrates dissolved during 17h acid hydrolysis (AH).*

	Ara (%)	Gal (%)	Glu (%)	Xyl (%)	Man (%)
Pine:					
FT-Kraft pulp	6.6	1.4	74.5	2.4	21.0
Kraft pulp *17h AH*	1.4	1.5	73.9	2.8	20.5
4h AH	4.9	3.2	48.2	14.8	28.8
PS-AQ pulp	1.0	1.8	69.7	1.7	25.8
Birch:					
FT-Kraft pulp	-	-	93.3	5.7	1.1
Kraft pulp *17h AH*	-	0.2	91.7	6.9	1.1
4h AH	-	0.4	54.4	43.8	1.4
PS-AQ pulp	0.4	1.1	87.6	5.8	5.2

3.1.2.2. Comparison between pine and birch pulps

According to the $CrI_{CPMAS+AH}$ values, the cellulose crystallinity is lower in birch pulps than in the corresponding pine pulps. It has been reported earlier that in hardwoods the degree of crystallinity is slightly lower than in the softwoods,[78] which seems to remain also after pulping.

As already mentioned, the CrI_{PSRE} values of birch pulps are even lower than the corresponding $CrI_{CPMAS+AH}$ values. This is a result of the incomplete removal of xylan from birch pulps by the PSRE-method, and the xylan signal can still be seen at 82 ppm in the subspectrum of the crystalline component (Fig. 3-1). This indicates a similar relaxation behaviour of xylan and cellulose, which may be a consequence of a close association and interactions between xylan and cellulose, or increased relaxation times of xylan due to the ordered structure.[84] It has been suggested earlier that the less substituted xylan dissolved during pulping resorbs into fibre and may be deposited on the surface of cellulose fibrils, interacting with cellulose and having a well ordered ultrastructure.[73,79,84] Recently, the presence of an inaccessible xylan within cellulose fibril aggregates has also been suggested.[81] Both factors may contribute to the incomplete removal of xylan by the PSRE-method observed in this study.

Correspondingly, all the glucomannan could not be removed completely by the PSRE method. The C1 signal of mannose residues can still be seen at 102 ppm in the subspectra of the crystalline components of all the softwood pulps studied in this thesis (Figure 2-3). It is therefore likely that some of the glugomannan may as well possess an ordered ultrastructure or interact with cellulose. However, this is probably not as extensive as in the case of xylan in hardwood pulps, since no significant decrease in the CrI_{PSRE} values was observed, although crystalline mannan has also been reported to resonate at the amorphous region (81.4 ppm).[80] Similar observations on glucomannan with a well-ordered structure have also been reported in wood.[83,99]

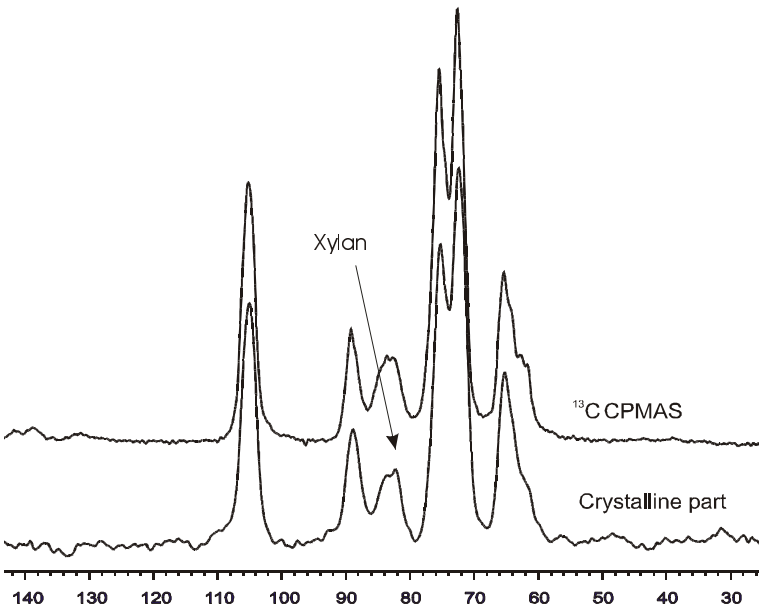

Figure 3-1. *^{13}C CPMAS spectrum and separated subspectrum of the crystalline part of birch kraft pulp.*

In the relative proportions of cellulose polymorphs, no significant differences could be observed between the pine and birch pulps (Table 3-4). The minor differences detected are within the error margin of the combined resolution enhancement and deconvolution method. Although in hardwoods the content of cellulose I_α has been shown to be lower than in the softwoods,[82,I] this difference is averaged out during pulping and a similar amount of cellulose I_α survives both in pine and birch pulps without conversion into cellulose I_β.

Table 3-4*. The relative proportions of cellulose polymorphs in ECF-bleached pine and birch pulps.*

	Cellulose Iα (%)	**Cellulose Iβ (%)**	**Cellulose II (%)**
Pine:			
FT-Kraft	27	64	9
Kraft	35	56	9
PS-AQ	36	55	9
Birch:			
FT-Kraft	35	54	11
Kraft	37	52	11
PS-AQ	36	50	14

3.1.2.3. Comparison between FT-Kraft, conventional kraft and PS-AQ pulps

After the spectroscopic or chemical removal of hemicelluloses no significant differences in the cellulose crystallinities were observed between pulps obtained by various pulping methods (Table 3-2). No differences in the relative proportions of cellulose polymorphs were detected either (Table 3-4). Only in the pine FT-kraft pulp does the proportion of cellulose I_α seem to be lower than in the other pulps. However, any enhanced transformation of cellulose I_α into cellulose I_β was not observed for the FT-kraft pulp of birch.

3.1.3. Comparison of fines and long fibre fractions of spruce kraft pulp
(Papers II, III & IV)

The structure of the fibre wall is inhomogeneous and the composition of the fibre surface differs from the rest of the fibre. In order to obtain information on the effects of kraft pulping on the fibre surface structure, kraft pulp was refined and the fibrillated surface material (fines) was separated from the long fibres.

In paper II, kraft pulp was refined in water and in weakly alkaline (0.01 M NaOH) media before separation of fines and long fibre fractions. The fines fractions obtained this way contain thus also ray cells, although their amount is quite small.

In Paper III, the fibre surface structure was investigated more closely by sequential refining (Fig. 3-2). This time the primary fines were isolated from the long fibres of the original kraft pulp already before refining. The long fibres obtained after the removal of the primary fines were then refined three times, and after each refining stage the fines were removed before the next refining step. The primary fines are known to contain mostly ray cells and some

fibrillated material, whereas secondary fines contain mostly fibrillated material from the fibre surface with some ray cells.[57,62,135] Due to the sequential refining, the fibrillated surface material of the secondary fines is believed to represent surface fractions from the deeper fibre surface layers after each refining step.

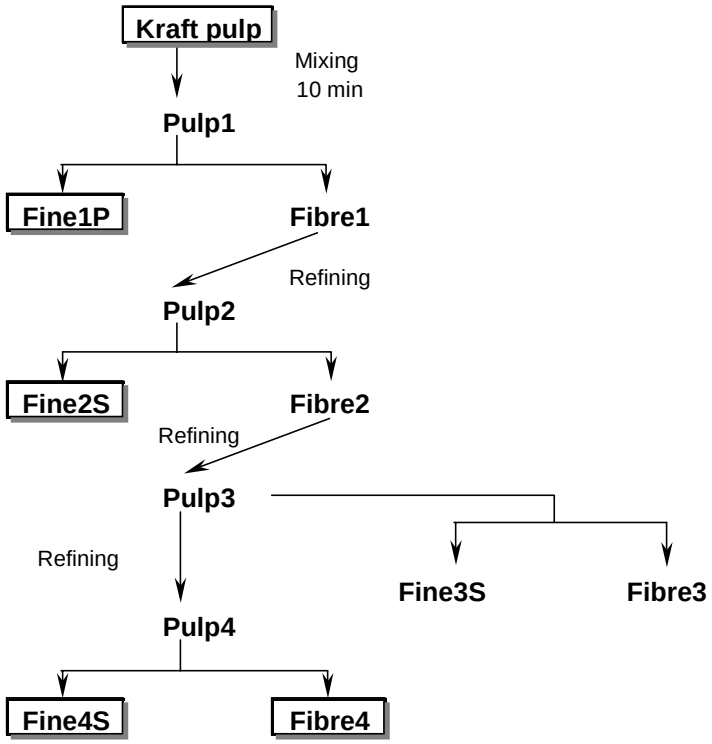

Figure 3-2. *Separation of fines and long fibre fractions by sequential refining.*[III]

3.1.3.1. Crystallinity of cellulose *(Papers II, III & IV)*

Refining of kraft pulp in water or in weak alkali was not observed to affect the crystallinity of cellulose according to the ordinary ^{13}C CPMAS measurements.[II] This is consistent with the results of Lennholm.[136] However, the cellulose crystallinity of fines (37-40%) was found to be clearly lower than in the kraft pulp or in the long fibre fractions (48-51%). In addition, the fines fractions were found to contain higher amounts of lignin, hemicelluloses and extractives. In fines fractions of sequential refining the contents of hemicelluloses, lignin and extractives were found to decrease gradually from Fine1P towards Fine4S accompanied with increased crystallinity.[III]

In order to confirm that the lower CrI_{CPMAS} values detected for fines are not only due to the higher amount of lignin and hemicelluloses, the crystallinity of cellulose in fines and fibre fractions obtained by sequential refining was determined also after spectroscopic (CrI_{PSRE}) and chemical ($CrI_{CPMAS+DL+AH}$) removal of amorphous lignin and hemicelluloses.[III,IV] The results obtained are presented in Table 3-5.

Table 3-5. *Cellulose crystallinities determined before (CrI_{CPMAS}) and after the chemical removal of lignin and hemicelluloses ($CrI_{CPMAS+DL+AH}$) by ordinary ^{13}C CPMAS as well as by the PSRE method (CrI_{PSRE}), together with the relative proportions of cellulose polymorphs for fines and long fibre fractions of sequential refining.*

	Glucose content[1](%)	CrI_{CPMAS} (%)	CrI_{PSRE} (%)	$CrI_{CPMAS+DL+AH}$ [2] (%)	Cellulose Iα (%)	Cellulose Iβ (%)	Cellulose II (%)
Kraft pulp	83.7	49	68 (3)[3]	- (59)[4]	28	64	8
Fine1P	78.7	38	61 (3)	60 (56)	21	66	13
Fine2S	83.0	41	57 (1)	62 (58)	26	67	7
Fine4S	83.8	44	63 (2)	- (58)	25	64	11
Fibre4	84.6	51	71 (3)	65 (60)	29	64	7

[1]Glucose content in relation to other monosaccharides, [2] DL = $NaClO_2$ delignification, 4h at 70°C, AH = 17h acid hydrolysis by 2.5M HCl at 100°C, [3] standard deviation, [4] crystallinities determined in STFI with a different spectrometer and peak fitting program.

After the spectroscopic removal of non-cellulosic components, the cellulose crystallinity of fines (57-63%) was still found to be clearly lower than in the original pulp (68%) or in the long fibres (71%), indicating lower cellulose crystallinity in ray cells and on the outermost fibre surface. This is in accordance with earlier results, according to which cellulose crystallinity is lower in ray cells and in the primary wall compared to the secondary wall.[137-138] However, no clear gradient in cellulose crystallinity between various fines fractions could be detected by the PSRE-method, in contrast to the CrI_{CPMAS} results.

Similarly, a difference in the cellulose crystallinity between fines (60-62%) and long fibres (65%) was observed also after acid hydrolysis, although in this case the difference is not as large as that obtained by the purely spectroscopic PSRE-method. This is probably due to the disadvantageous effects of the acid hydrolysis, as discussed in section 3.1.2.1. The dissimilarity in $CrI_{CPMAS+DL+AH}$ values obtained in our laboratory and in STFI is most likely a consequence of the differences in the spectral fitting methods. However, the trends in CrI values obtained by both laboratories are similar.

No significant difference in the relative proportions of cellulose polymorphs was observed between fines and long fibre fractions, indicating that the relative proportions of cellulose polymorphs remain similar throughout the entire fibre radius and is similar also in the ray cells.

3.1.3.2. Lateral dimensions of fibrils and fibril aggregates *(Paper IV)*

Since the surface material of the cellulose crystallites resonates in the same spectral region as the amorphous C4 signal used to determine the CrI, the lower degree of crystallinity in fines may be an indication of smaller fibril size in ray cells and on the fibre surface. Therefore, the average lateral fibril (LFD) and fibril aggregate dimensions (LFAD) were determined as described in section 2.1.1.4. [IV] In order to obtain quantitative cellulose spectra, the lignin and hemicelluloses were removed by $NaClO_2$ delignification (4h at 70°C) and prolonged acid hydrolysis (17h in 2.5M HCl at 100°C).

Table 3-6. *The average lateral fibril (LFD) and fibril aggregate dimensions (LFAD) for the kraft pulp, the fines fractions and the long fiber fraction.*

	LFD (nm)	**LFAD (nm)**
Kraft pulp	4.9 (0.2)[1]	17.0 (0.9)[1]
Fine 1P	4.5 (0.2)	17.8 (1.4)
Fine 2S	4.8 (0.2)	17.8 (1.4)
Fine 4S	4.9 (0.2)	17.9 (1.7)
Fiber 4	5.0 (0.2)	19.4 (1.1)

[1] Standard error

According to the results shown in Table 3-6, the average lateral fibril dimensions in the secondary fines (4.8-4.9 nm) and in the long fibre fraction (5.0 nm) are almost equal within the limits of statistical error. Only in primary fines is the LFD slightly lower (4.5 nm) than in the other fractions. This may be an indication of the slightly smaller fibril dimensions of ray cells, but on the fibre surface fibril width is similar to that inside the fibre.

In the refined long fibre fraction the average lateral fibril aggregate dimension is slightly higher (19.4 nm) than in the original pulp (17.0 nm) or in the fines fractions (17.8-17.9 nm). It has been shown earlier that LFAD increases during kraft pulping and drying.[139] In both cases the lower hemicellulose content correlates with the higher tendency for aggregation due to the increased contact between cellulose fibril surfaces. Swelling has also been suggested to facilitate the rupture of hemicellulose-hemicellulose and hemicellulose-cellulose associations during kraft pulping, resulting in an increase in non-hindered accessible cellulose fibril surfaces and further aggregation via the formation of interfibrillar hydrogen bonds and van der Waals forces.[139] The present results are consistent with these findings, and the increase observed in LFAD of the long fibre fraction is probably a consequence of the extensive multistage refinement. As a result of the refining, the fibre wall is fractured and some of the surface material is removed. This allows better swelling of the refined long fibres in water and an improved mobility of the cellulose chains, which can lead to a further fibril aggregation during drying. In fines the amount of hemicelluloses is higher, thus reducing the aggregation.

3.1.4. Effects of TCF-bleaching and refining *(Paper II & some unpublished data)*

Another objective of refining was to test its capability to activate the kraft pulp towards a better tendency for bleachability. The effect of refining and TCF-bleaching on the cellulose crystallinity was investigated by ordinary ^{13}C CPMAS measurements for the original kraft pulp, as well as in water (Pulp1) and in weak alkali (0.01 M NaOH) refined kraft pulp (Pulp3) after the O-delignification stage and the OQPZP-bleaching sequence (Table 3-7)[II].

According to the CrI_{CPMAS} values, refining or TCF-bleaching have no significant effect on the cellulose crystallinity.[II] However, since a slight increase could be seen after the oxygen delignification stage in the CrI of kraft pulp refined in water (Pulp1O), the effect of TCF-bleaching and refining on the cellulose crystallinity was later investigated more closely also by the PSRE-technique.

Table 3-7. *The crystallinity indices determined by the ordinary ^{13}C CPMAS (CrI_{CPMAS}) and PSRE (CrI_{PSRE}) methods, together with the relative proportions of cellulose polymorphs for kraft pulp and refined pulps (Pulp1, Pulp3) before and after the O-stage and OQPZP-bleaching.*

	Viscosity (ml/g)	**CrI_{CPMAS} (%)**	**CrI_{PSRE} (%)**	**Iα (%)**	**Iβ (%)**	**II (%)**
Kraft pulp	1300	50	68 (3)	26	64	10
Pulp1	1290	50	73 (2)	31	57	12
Pulp3	1260	50	73 (1)	33	58	9
PulpO	1050	48	75 (1)	26	62	12
Pulp1O	1030	53	78 (1)	30	59	11
Pulp3O	1030	48	78 (2)	29	59	12
PulpOQPZP	640	49	73 (2)	26	59	15
Pulp1OQPZP	620	51	75 (1)	30	59	11
Pulp3OQPZP	690	48	73 (2)	28	62	10

O=oxygen, Q=EDTA, P=H_2O_2, Z=O_3,

The CrI_{PSRE} results show that both refining and oxygen delignification have a slight increasing effect on the cellulose crystallinity, and for the refined pulps the increase in cellulose crystallinity during oxygen delignification is even more pronounced. During the rest of the TCF-bleaching sequence, the degree of cellulose crystallinity decreases slightly. However, either refining or TCF-bleaching was not found to have any effect on the relative proportions of cellulose polymorphs.

Cellulose crystallinity has been reported to increase during drying due to the removal of residual distortions in the interior of cellulose fibrils.[104,140] The increase in the cellulose crystallinity during drying may be facilitated in refined fibres due to their better ability to swell in water or in dilute alkali, as was suggested also in the case of increased LFAD values of refined fibres. Increased mobility of the cellulose chains in the swollen state may improve the reorientation of the chains parallel to the crystallites nearby.

Oxygen delignification is known to have a limited selectivity, especially towards the end of delignification, and the degradation of cellulose during the O-stage and OQPZP-sequence can be seen as a lowering of viscosity (Table 3-7). Cellulose degradation during oxygen delignification occurs mainly by alkali driven peeling and by cleavage of glycosidic linkages through oxidation.[4,5] Since disordered cellulose is more susceptible to degradation, the proportion of the crystalline cellulose increases. In addition to the removal of more accessible amorphous cellulose, a random cleavage of glycosidic bonds in crystallite defects and accessible surfaces may take place, leading to the loosening of chain-ends from the crystalline domain and to the disordering. Both of these degradation mechanisms have been suggested to take place during oxygen delignification,[141] but due to the preferential degradation of amorphous cellulose, the proportion of crystalline cellulose increases during oxygen delignification.

During the QPZP-sequence, similar carbohydrate degradation reactions take place. In this case the degradation of cellulose at the crystallite defects and accessible surfaces is probably more extensive than the removal of amorphous cellulose, and the net effect is the slight disordering of cellulose.

3.2. Lignin structure

3.2.1. Effects of kraft pulping and oxygen delignification *(Papers V & VII)*

The effect of kraft pulping and oxygen delignification on the structural features of lignin was investigated by ^{13}C CPMAS in the solid state.[V] More detailed effects of kraft pulping and oxygen delignification on the lignin side-chain structure were investigated by modern 2D HSQC and 3D HSQC-TOCSY measurements in solution.[VII] Spruce milled wood lignin (MWL), lignin dissolved during kraft pulping (Kraft-SLL) as well as residual lignins of unbleached (Kraft-RL) and oxygen delignified (KraftO-RL) kraft pulps were compared.

3.2.1.1. Effects on the structural features of lignin *(Paper V)*

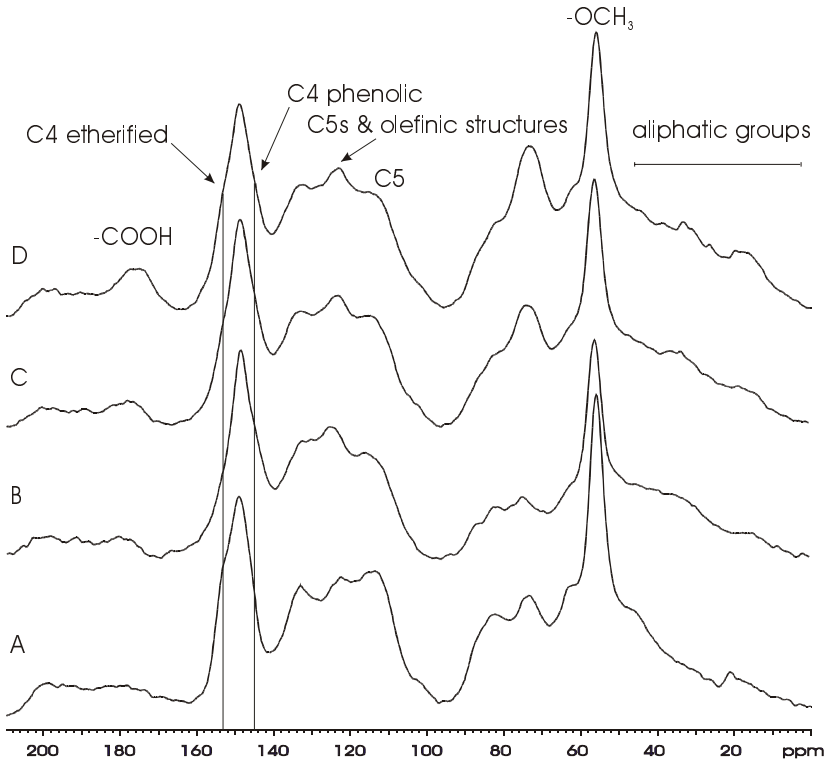

Figure 3-3. *The ^{13}C CPMAS spectra of a) MWL, b) dissolved kraft lignin and residual lignins of c) unbleached and d) oxygen delignified kraft pulp.*

In kraft pulping, lignin is mostly removed by the cleavage of β-O-4 aryl ether linkages. This can be seen in the CPMAS spectra of softwood lignin as a variation in the shape of the C3 and C4 signal (140-160 ppm). The etherified lignin units, mainly representing β-O-4 linkages, can be seen as a shoulder at 153 ppm, whereas the phenolic lignin units resonate on the other side of the same signal at 145 ppm.[97] According to the CPMAS spectra shown in Figure 3-3, the dissolved kraft lignin contains mostly phenolic guaiacyl groups, although some of the β-O-4 structures also survive. In the residual lignin the amount of β-O-4 linkages is lower than in the MWL but still higher than in the dissolved kraft lignin. During oxygen delignification, the relative content of the aryl ether bonds was found to increase again due to the preferential removal of phenolic guaiacyl units. The content of carboxylic

acid groups (170-180 ppm) in the residual lignin also increases during the oxygen delignification, which is most likely due to the formation of muconic acid groups.

Condensation reactions are likely to occur during kraft pulping, since in the spent liquor lignin and in the residual lignins the signal intensity of protonated C5 carbons (116 ppm) is lower than in MWL. The substitution of C5 carbons as well as the formation of stilbenes from β-5 structures can be seen as an increase of intensity in the region of 120-130 ppm. During the kraft pulping and oxygen delignification, the amount of aliphatic groups increases. Some of these groups may be due to the extractives or protein impurities of cellulase enzymes, but most likely this indicates the formation of saturated end-groups or some condensed lignin side-chain linkages. Demethoxylation can also be seen in a decreased intensity of the methoxyl signal at 56 ppm after kraft pulping.

3.2.1.2. Effects on lignin side-chain structures *(Paper VII)*

The lignin side-chain structures that were traced out on the basis of the 2D HSQC and 3D HSQC-TOCSY spectra are shown in Figure 3-4 and the expansions of side-chain areas of 2D HSQC spectra of MWL and Kraft-RL are presented in Figures 3-5 and 3-6.[VII]

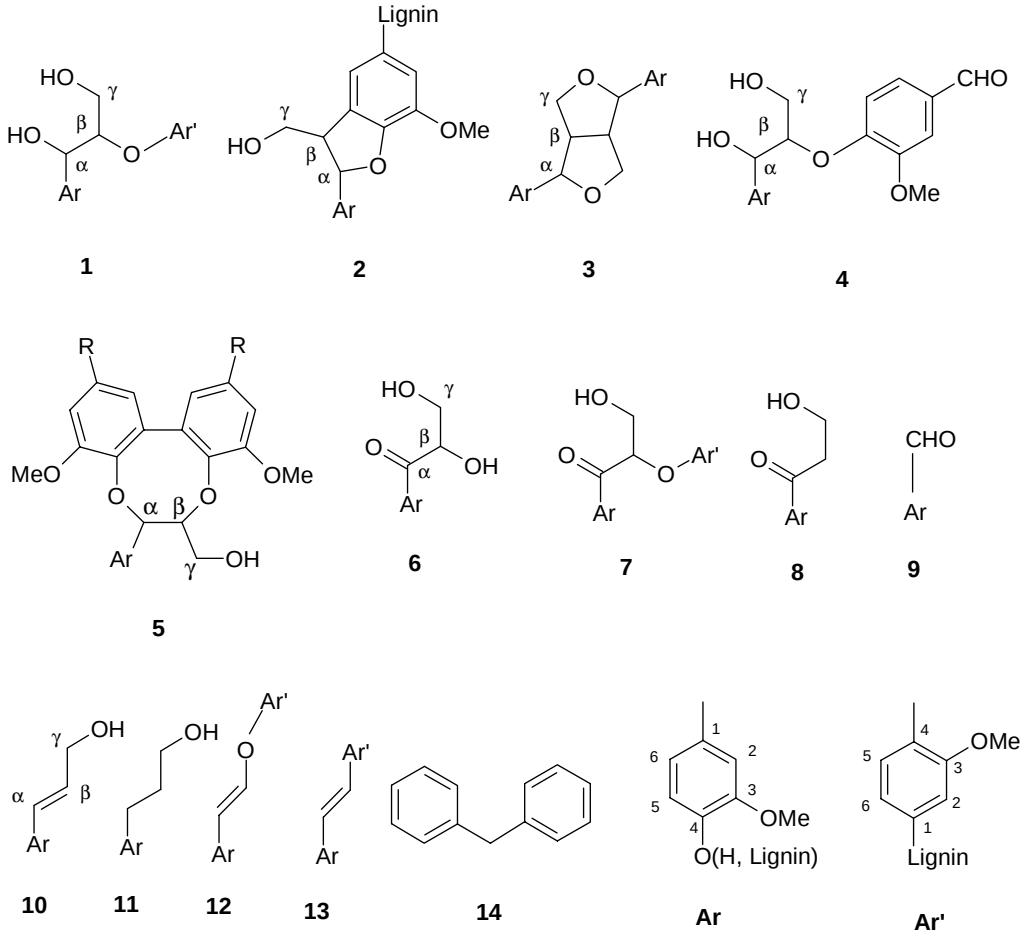

Figure 3-4. *Lignin side-chain structures assigned on the basis of the 2D HSQC and 3D HSQC-TOCSY measurements. The structures are referred to in the text by the corresponding numerals.*

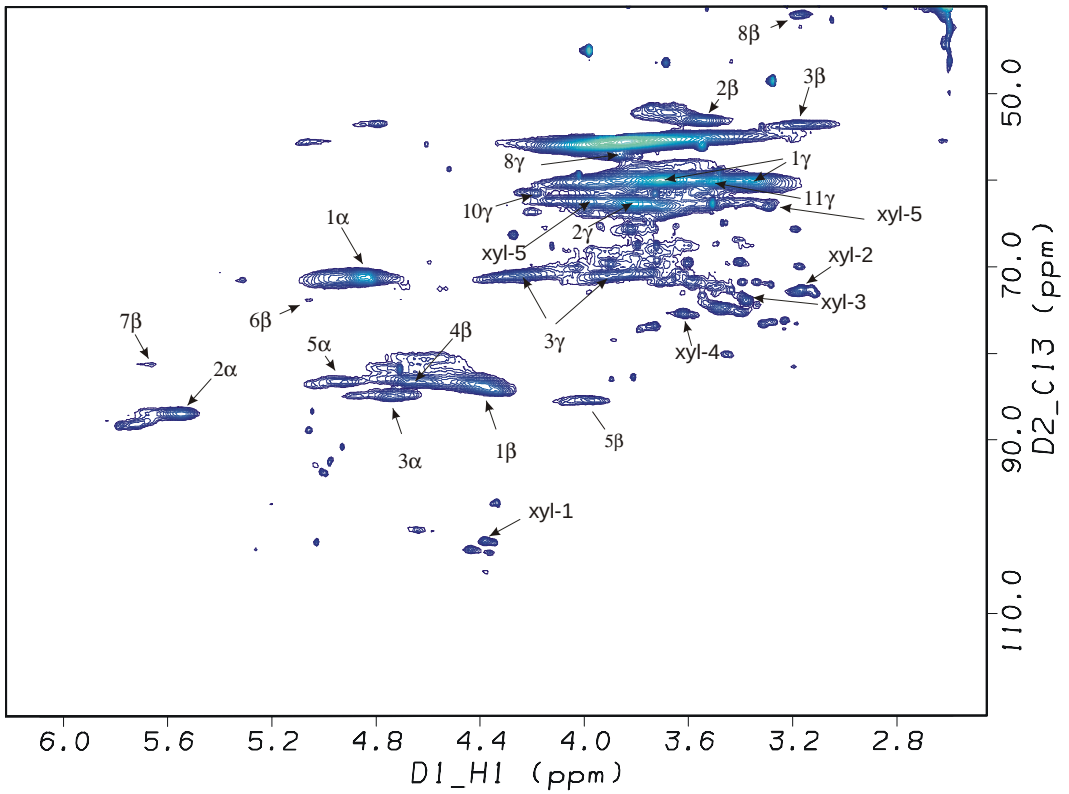

***Figure 3-5**. Expansion of the side-chain region of 2D HSQC-spectrum of MWL.*

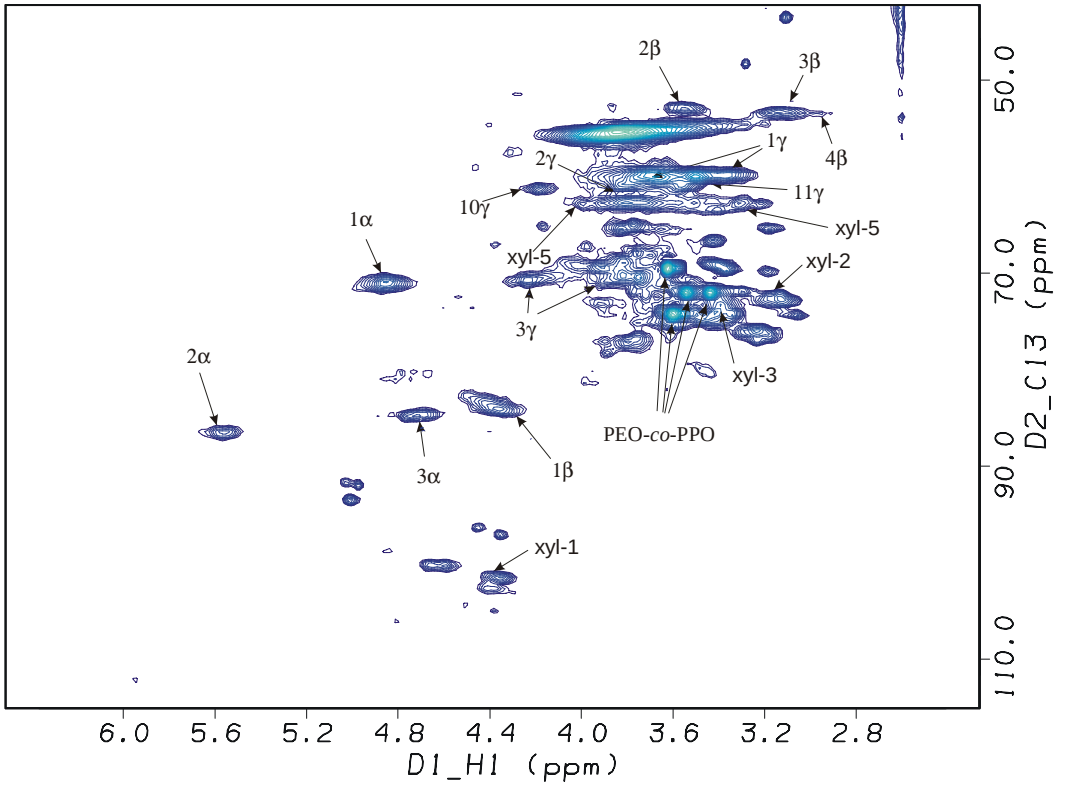

***Figure 3-6**. Expansion of the side-chain region of the 2D HSQC-spectrum of Kraft-RL.*

According to the 2D HSQC and 3D HSQC-TOCSY measurements, most of the original structures identified in MWL are still present in technical lignins, although their relative proportions vary after kraft pulping and oxygen delignification. The dominant side-chain linkages in all lignin samples are the β-aryl ether (β-O-4, **1**), the phenyl coumaran (β-5, **2**) and the pinoresinol (β–β, **3**) structures (Figure 3-4). The cleavage of aryl ether linkages during kraft pulping can be seen as a decrease in the relative amounts of β-O-4 and β-5 structures in Kraft-SLL and Kraft-RL (Table 3-8), whereas the β–β structures are more stable in the kraft pulping conditions. In the spent liquor lignin the cleavage of β-O-4 and β-5 linkages is slightly more extensive than in the residual lignin, which is in accordance with the solid-state NMR spectroscopic studies. The *erythro* forms of β-O-4 structures were found to be more reactive in kraft pulping conditions than the corresponding *threo* forms, as has been reported also earlier.[10-13] Due to the preferential removal of phenolic lignin units[19-20] the amount of β-O-4 linkages increased during the oxygen delignification, in relation to the β–β structures. The proportion of α-aryl ether linkages containing β-5 structures also increased slightly in relation to the β–β structures.

Table 3-8. *The relative signal intensities of β–O–4, β–5 and β–β structures in MWL, Kraft-SLL, Kraft-RL and KraftO-RL according to their α-correlations in HSQC-spectra.*

	MWL	**Kraft-SLL**	**Kraft-RL**	**KraftO-RL**
β–O–4	5.4	1.2	1.9	4.4
β–5	2.4	0.6	0.8	1.2
β–β	1.0	1.0	1.0	1.0

Dibenzodioxocin structures have been reported to be very reactive under the kraft pulping conditions,[14,15] but some traces of *trans*-dibenzodioxocin (**5**) structures could still be detected in the spent liquor lignin and in the residual lignin, although they are not seen in Figure 3-5 due to their low intensities. After oxygen delignification, the dibenzodioxocin structures could no longer be found.

The α-carbonyl structures (**4, 6, 7, 8**) observed in MWL were not detected in any technical lignins. The absence of structures (**4**) and (**7**) in technical lignins is expected, since the alkaline cleavage of β-aryl ether bonds in non-phenolic lignin units is known to be accelerated by the α-carbonyl groups.[8,9] The absence of α-carbonyl structures in KraftO-RL is, however, inconsistent with the earlier UV-results, according to which the amount of α-conjugated structures increases during oxygen delignification.[142] Since the α-carbonyl carbon is not protonated, the correlation of this carbon cannot be obtained directly from the 2D HSQC or 3D HSQC-TOCSY spectra. However, benzaldehyde (**9**) structures were found in KraftO-RL, which is consistent with the UV-results. It is also well known that benzaldehyde structures are formed in oxygen delignification conditions by the cleavage of conjugated double bonds.[19-21]

The number of saturated aliphatic groups was found to increase during kraft pulping and oxygen delignification. Coniferyl alcohol (**10**) and dihydroconiferyl alcohol (**11)** end groups were detected in all lignins, but in the technical lignins the content of these structures seems to be higher. Coniferyl alcohol structures are known to be formed in kraft pulping conditions and they have been shown to form new carbon-carbon linkages between the side chains, as

well as undergoing various disproportionation reactions forming lower molecular weight products with aliphatic side-chain structures.[143] The dihydroconiferyl alcohol structure is one of these disproportionation products of coniferyl alcohol.

Enol ether, i.e. vinyl aryl ether, structures (**12**) may be formed to some extent during the kraft pulping as a result of alkali-promoted elimination of γ-hydroxymethyl groups from β-O-4 structures in the absence of hydrosulphide ions, but any reliable evidence of these structures could not be found in any technical lignins. Stilbene (**13**) structures are also known to be formed during kraft pulping, mainly by the cleavage of the α-aryl ether bond of phenylcoumaran (β-5) (**2**) structures. Correlations suitable for stilbene structures were observed in both Kraft-SLL and Kraft-RL.

Although diphenyl methane (DPM) structures (**14**) have been suggested to form to some extent during kraft pulping by condensation reactions,[45] these structures could not be detected in any of the technical lignins. Therefore, the higher content of condensed structures found in residual lignins on the basis of the CPMAS measurements is not due to the formation of DPM structures.

In addition to these lignin structures, a very intense spin-system whose ^{1}H-^{13}C correlations resonate at 1.15/16.9, 3.44,3.54/72.0, 3.6/74.3 and 3.62/69.5 ppm, was found in both residual lignins. According to the HMBC (Heteronuclear Multiple Bond Correlation) and DEPT (Distortionless Enhancement by Polarization Transfer) measurements, as well as the corresponding measurements conducted on a commercial reference polymer, this spin-system was assigned for poly(ethylene oxide-*co*-propylene oxide). Chemical shifts represented in the literature for the corresponding polymer also support this proposal.[144] However, the exact origin of this structure is not known.

3.2.2. Residual lignin structure in fines and long fibre fractions of kraft pulp *(Papers III & V)*

According to the CPMAS measurements, refining was not observed to cause any changes in the structure of residual lignins.[V] No significant structural differences between the residual lignins of primary and secondary fines or long fibres were found on the basis of their CPMAS spectra either.[III] Only a slightly higher degree of etherification (Fig. 3-7) as well as the extent of condensation (Fig. 3-8) were detected in the residual lignin of fines compared to the corresponding residual lignin of the fibre fraction.[III] This indicates a less phenolic and more condensed nature of lignin in ray cells as well as in the middle lamella and primary wall compared to the secondary wall lignin, which is consistent with the results for spruce wood. [52-55]

In the residual lignin fractions of fines the amount of carbohydrates was found to be higher than in the corresponding residual lignin fractions of long fibres,[III,V] as will be discussed in greater detail in section 3.3.1. Also the extractives were found to enrich in residual lignin fractions of fines.

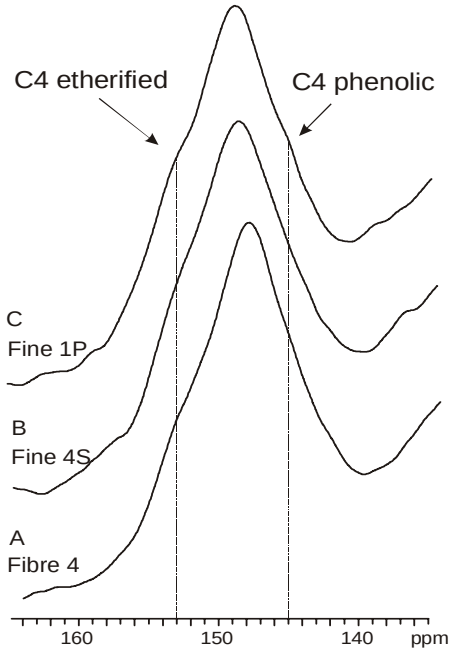

Figure 3-7. *Expansion of the C4-region in ^{13}C CPMAS spectra of residual lignins isolated from a) primary fines, b) secondary fines and c) long fibres.*[III]

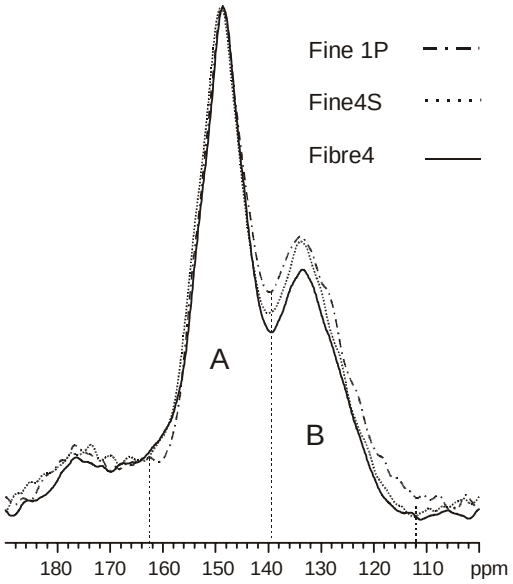

Figure 3-8. *Aromatic region of the dipolar dephasing spectra of residual lignins isolated from Fine1P, Fine4S and Fibre4.*[III]

3.2.3. Extent of lignin condensation *(Paper VI)*

Since condensed lignin structures have been suggested to be one factor that may contribute to the incomplete delignification, the extent of substitution in the aromatic ring of quaiacyl group was investigated by dipolar dephasing based methods in various technical lignins, as was described in section 2.1.2.1.[VI]

3.2.3.1. Condensed lignin structures in softwoods

As a representative of native lignin, pine (*Pinus sylvestris*) MWL was used together with lignin isolated enzymatically from ball milled spruce (*Picea abies*) wood (MW-E).

Table 3-9. *The extent of aromatic substitution (f^H) and the average number of protonated aromatic carbons (CH_{number}) in native lignins.*

	f^H	Std (%)	CH_{number}	Condensed structures (%)
MWL (*Pinus sylvestris*)	0.430	2.1	2.6	42
MW-E (*Picae abies*)	0.393	1.5	2.4	64

According to the results shown in Table 3-9, spruce lignin isolated enzymatically from ball milled wood (MW-E), and thus considered to be a better representative of native lignin, was found to be more condensed than pine MWL. It is therefore probable that MWL represents

the most easily isolated and the least condensed part of lignin. Since MWL has been suggested to origin mostly from the secondary wall,[145-147] these results indicate that the native lignin in the other constituents of the cell wall is more condensed than in the secondary wall. This is consistent with earlier results, according to which lignin structure is more condensed in the middle lamella and in ray cells compared to secondary wall lignin.[51,55]

3.2.3.2. Effect of pulping

In order to investigate the effect of pulping on the extent of condensation, spruce lignin dissolved during kraft pulping (Kraft-SLL) and the corresponding residual lignin (Kraft-RL) were analysed. Pine lignin dissolved in various stages during the flow-through kraft cooking (FT-SLL 60 min, 120 min, 180 min and 240 min) and the corresponding residual lignin (FT-RL) were also studied together with the spent liquor lignin (Soda-AQ-SLL) and residual lignin (Soda-AQ-RL) of soda-AQ cook. The residual lignin of primary and secondary fines (Prim. Fine-RL, Sec. Fine-RL) and long fibre (Fibre-RL) fractions isolated before and after the refining of the conventional spruce kraft pulp were also compared.

Table 3-10. *The extent of aromatic substitution (f^H) and the average number of protonated aromatic carbons (CH_{number}) in technical lignins.*

	Kappa number	f^H	Std (%)	CH_{number}	Condensed structures (%)
FT-SLL-60	-	0.433	1.2	2.6	40
FT-SLL-120	-	0.423	2.1	2.5	46
FT-SLL-180	-	0.422	2.4	2.5	47
FT-SLL-240	-	0.398	2.3	2.4	61
FT-RL *pro RL*[1]	27	0.383	0.8	2.3	70
Kraft-SLL	-	0.379	3.0	2.3	73
Kraft-RL *pro RL*	36	0.375	1.8	2.3	75
Fibre-RL *pro RL*	-	0.375	0.8	2.3	75
Fibre-RL *pro is*[2]	-	0.397	3.4	2.4	62
Sec. Fine-RL *pro is*[3]	-	0.391	10.4	2.3	65
Prim. Fine-RL *pro is*[3]	-	0.370	3.7	2.2	78
Soda-AQ-SLL	-	0.412	2.0	2.5	53
Soda-AQ-RL *pro RL*	37	0.387	1.4	2.3	68

[1] The distinction of *pro RL* and *pro is* fractions is explained in Appendix 2. [2] The large amount of carbohydrates interferes. [3] Using narrower area (109-160 ppm) for integration an attempt was made to reduce the effect of carbohydrates.

According to the results shown in Table 3-10, all the technical lignins are more condensed than MWL. Studies of the black liquor lignins obtained as a function of time during the flow-through kraft cook show that the amount of condensed structures increases as the cook proceeds. This indicates that the uncondensed lignin structures are most easily removed already at the beginning of the cook. As the cook proceeds more condensed lignin structures

are dissolved. This supports the general assumption that the cooking chemicals are transferred from the lumen through the cell wall towards the middle lamella,[1,3] and the less condensed lignin of secondary wall is dissolved first, whereas the more condensed middle lamella lignin is dissolved last. Since the residual lignin remaining in the fibre is most condensed, it is also probable that the condensed lignin structures are less reactive throughout the fibre wall and are therefore enriched in the fibre. This is consistent with the results according to which the residual lignin of primary fines representing mainly the ray cells is only slightly more condensed than the residual lignin of long fibres or secondary fines, representing the secondary and the primary wall, respectively (Fig.3-8 & Table 3-10).[III,VI]

In the residual lignins of the conventional and flow-through kraft cook, the extent of condensation seems to be quite similar. The spent liquor lignin of conventional kraft pulp is, however, more condensed than the last SLL-fraction of the FT-cook, indicating that either more condensed lignin structures have been dissolved in the conventional kraft cook, or some further condensation has occurred in the black liquor lignin during the conventional cook.

The residual lignin of soda-AQ pulps was found to be nearly as condensed as the residual lignins of conventional kraft and FT-kraft pulps, but the spent liquor lignin of soda-AQ cook was found less condensed than the other black liquor lignins. It is therefore possible that the lignin dissolved in soda-AQ pulping is less condensed or the condensation reactions are more probable during the kraft pulping. However, this may also be an indication of anthraquinone residues, which have an increasing effect on f^H values due to their more protonated nature. Although the amount of anthraquinone is most likely very small, the exact effect of anthraquinone on these results is not known in detail.

3.2.3.3. Effects of oxygen delignification and peroxide bleaching

In order to investigate the effect of bleaching on the extent of lignin condensation, residual lignins isolated from the oxygen delignified (KraftO-RL) and peroxide bleached kraft pulps (KraftOQP-RL) were analysed. Furthermore, these were compared with the residual lignin of a super batch pulp cooked into a kappa number close to the pulps delignified by OQP-bleaching.

Table 3-11. *The extent of aromatic substitution (f^H) and the average number of protonated aromatic carbons (CH_{number}) in residual lignins of semibleached pulps.*

	Kappa number	**f^H**	**Std (%)**	**CH_{number}**	**Condensed structures (%)**
Kraft-RL *pro RL*	36	0.375	1.8	2.3	75
KraftO-RL *pro RL*	17	0.356	1.8	2.1	87
KraftOQP-RL *pro RL*	9	0.346	3.9	2.1	92
Super Batch *pro RL*	11	0.346	1.7	2.1	92

Oxygen delignification was found to further increase the relative amount of condensed structures in the residual lignin. A slight increase in the amount of condensed structures was

observed also after peroxide bleaching, but this is not as prominent as in the case of oxygen. Based on these results, it is reasonable to assume that the condensed lignin structures are more resistant towards oxygen delignification and accumulate into fibres during the oxygen delignification. The poor reactivity of the condensed 5-5'-biphenyl structures has been shown with model compounds, [23] but the formation of new condensed structures cannot be excluded, since in the same study it was shown that biphenyl formation may also take place during oxygen delignification.[23] Our present results, which include both phenolic and non-phenolic lignin units are consistent with earlier suggestions based on both the oxidative degradation[44,46] and ^{31}P NMR spectroscopic[22,43] analyses, involving only the phenolic lignin counterpart.

The residual lignin of unbleached super batch pulp with a low kappa-number was found to be as condensed as the residual lignin of OQP-bleached pulp of nearly the same kappa-number. This indicates that the degree of condensation of the lignin remaining in pulp is not dependent on the path of delignification, but the condensed structures seem to accumulate into the fibres during pulping as well as during the OQP-bleaching sequence.

3.3. Lignin-carbohydrate complexes

Linkages between lignin and carbohydrates have been suggested to be a major obstacle to complete delignification. Therefore, interactions between lignin and carbohydrates were investigated in the enzymatically isolated residual lignin samples by 2D solid-state HETCOR as well as by proton spin-lattice relaxation measurements.

3.3.1. RLCCs observed indirectly by ^{13}C CPMAS *(Paper III & V)*

The enzymatic hydrolysis used to isolate residual lignins was followed by protease purification, after which a NaOH soluble *pro RL* and an insoluble *pro is* fraction of the residual lignins were obtained (Appendix 2). In the insoluble *pro is* and *pro isis* fractions a clear carbohydrate signal can be seen also at 105 ppm, whereas in the other fractions carbohydrate signals are overlapped with the lignin signals, and therefore impossible to analyse. This signal at 105 ppm was considered to indicate the presence of cellulose in all *pro is* and *pro isis* residual lignin fractions, despite the enzymatic hydrolysis.[III,V] Furthermore, the content of cellulose was found to be considerably higher in the *pro is* fractions of fines than in the corresponding fractions of long fibres. In the *pro is* residual lignin fraction of primary fines the relative proportion of cellulose was highest (Fig. 3-9).[III]

The cellulose that remains in the *pro is* residual lignin fractions was concluded to indicate strong interactions between the residual lignin and cellulose, which probably somehow prevent the complete enzymatic hydrolysis of cellulose and may as well contribute to the incomplete delignification during pulping. The observed interaction may be due to the covalent bonding or physisorption. On the basis of our results it cannot be concluded, whether the suggested LC-complexes are native or formed during the kraft pulping. On the basis of the methylation analysis, Iversen and Wännström[37] have reported the presence of alkali-stable lignin-carbohydrate bonds, mainly to cellulose, in the enzymatically isolated residual lignin of kraft pulp. They suggested that these bonds were formed during kraft pulping. However, the existence of similar enzymatically isolated lignin fractions from pine

wood containing a considerable amount of cellulose has also been reported, thus indicating at least partly the native origin of the suggested cellulose-lignin complexes.[148]

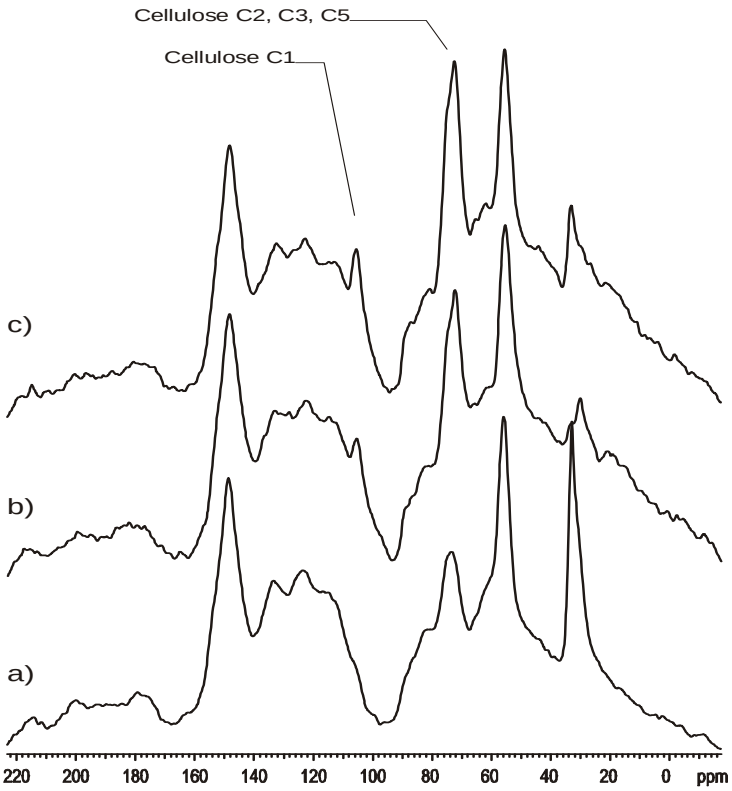

Figure 3-9. *The ^{13}C CPMAS spectra of the pro is fractions of residual lignins isolated from a) long fibre fraction, b) secondary fines and c) primary fines fractions of sequentially refined kraft pulp.*

3.3.2. Relaxation measurements

Attempts were made to determine proton spin-lattice relaxation times for the lignin and carbohydrate components of the residual lignins. The relaxation time of carbohydrate component could not, however, be determined reliably due to the low amount of carbohydrates present (~5-7%) and interfering lignin signals, which resonate in the same spectral region as carbohydrates (~60-100 ppm). The NMR measurements in solution showed that the suggested polymer structure resonates in the carbohydrate region as well. [VII]

Only in the insoluble *pro is* residual lignin fractions of fines, which contain high amounts of cellulose, could the signal at 105 ppm be used to determine the $T_{1\rho H}$-relaxation time for the carbohydrate component (Table 3-12). In these fractions, the $T_{1\rho H}$ relaxation times of lignin and carbohydrate components are very similar, indicating that spin-diffusion has been able to average out the relaxation times of cellulose and lignin. The components are thus homogeneous at the molecular level in the scale of few nanometers and do not form domains of their own.[120] This conclusion is supported by the fact that the lignin and cellulose components could not be separated into subspectra by the PSRE-method, which is based on the different $T_{1\rho H}$-relaxation times of the components.

Table 3-12. *Proton spin-lattice relaxation times in rotating frame for insoluble pro is residual lignin fractions of fines.*

Sample	$T_{1\rho H}$ for lignin component (ms)	$T_{1\rho H}$ for carbohydrate component (ms)
Fine1P *pro is*	7.1	7.0
Fine4S *pro is*	6.8	6.6

3.3.3. Solid-state HETCOR *(Paper V)*

The resolution of solid-state HETCOR measurements was not found to be good enough to investigate the interactions between lignin and carbohydrates. The HETCOR spectra of residual lignins show a through space correlation between aliphatic carbons (~74 ppm) and aromatic protons.[V] Because the carbohydrate carbons resonate approximately at 74 ppm and this correlation could not be seen in the spectra of MWL we reported, according to the preliminary measurements that this could be an indication of close association between aliphatic carbohydrates and aromatic lignin.[V] Further studies on lignin model compounds have proven, however, that this correlation can also be due to lignin structure, indicating rather the close proximity of the lignin side-chain carbons and the aromatic protons of lignin. The synthetic polymer contaminant found in solution NMR measurements[VII] also interferes with the HETCOR measurements.

4. CONCLUSIONS

Various NMR methods both in solid and liquid state were applied to investigate the effects of chemical pulping related processes on the polymeric components of wood and pulp. It was shown that the NMR methods used in this thesis are very well applicable to versatile studies of lignocellulosics. Especially the PSRE method based on delayed contact pulse sequence proved to be better in the removal of interfering hemicellulose signals from softwood pulp spectra before determination of CrI than the chemical removal of hemicelluloses by acid hydrolysis. However, all hemicellulose signals could not be removed from birch pulps by the PSRE method, and therefore birch pulps were suggested to contain larger amounts of well-ordered xylan. The dipolar dephasing method also proved to be a valuable method for determining the amount of condensed lignin structures. With this non-destructive method the relative amount of condensed lignin structures can be monitored both in phenolic and non-phenolic lignin units, and this determination is not dependent on the solubility of the sample. Most of the present results obtained by NMR methods support the previous suggestions for the various obstacles to delignification.

Solid-state NMR spectroscopic analyses showed that cellulose crystallinity increases during pulping. Due to the preferential removal of less ordered cellulose, a slight increase in cellulose crystallinity was also observed during oxygen delignification. During the QPZP-bleaching sequence the degree of cellulose crystallinity was found to decrease slightly as a result of more extensive cellulose degradation in the accessible parts of crystallites. Various pulping methods or hemicellulose contents were not observed to affect cellulose crystallinity, but after kraft pulping, the cellulose crystallinity was found to be lower in ray cells and on the fibre surface compared to the long fibre fractions. Refining was observed slightly to facilitate the cellulose fibril aggregation as well as crystallization, probably during drying due to the better swellability of the fibres and therefore improved mobility of cellulose chains.

Ordinary ^{13}C CPMAS measurements could be used to monitor some important features of the lignin structure. Modern 2D HSQC and 3D HSQC-TOCSY measurements in solution could be applied for more detailed structural studies of bonding patterns of lignin. Those studies reveal that most of the original structures identified in MWL are still present in technical lignins, although their relative proportions vary after kraft pulping and oxygen delignification. The cleavage of aryl ether linkages during kraft pulping and the preserving effect of oxygen delignification on aryl ether linkages were observed in both solid-state and in solution NMR studies. However, some reactive structures, e.g. β-O-4 and dibenzodioxocin structures were still found in residual lignin after kraft pulping and some of the reactive structures were shown to remain even in the dissolved spent liquor lignin. Similarly, residual lignin is still to a certain extent phenolic after oxygen delignification. It is therefore reasonable to assume that the reactivity of those functionalities is hindered, probably by their involvement with less reactive condensed structures or LC-complexes as has been suggested earlier.

According to the dipolar dephasing results, the condensed aromatic lignin structures are enriched into fibres during pulping and oxygen delignification, whereas the less condensed lignin structures are removed already in the early stage of pulping. However, the formation of new condensed structures cannot be excluded either, although the condensed diphenyl methane structures could not be found in residual lignins using multidimensional NMR measurements.

Due to the low amount of carbohydrates as well as the interfering lignin and PEO-co-PPO signals, the interactions between lignin and carbohydrates in residual lignins could not be investigated reliably by proton spin-lattice relaxation and HETCOR measurements. However, evidence of residual lignin-carbohydrate complexes was obtained indirectly by ordinary CPMAS measurements as well as by relaxation measurements in residual lignin fractions containing larger amounts of carbohydrates. According to these measurements, interactions between cellulose and lignin are possible. In ray cells and on the fibre surface those interactions are more prominent than in the fibres. Otherwise, no significant differences in the residual lignin structure between fines and long fibres were observed. The residual lignin of fines was found to be less phenolic and only very slightly more condensed than the residual lignin of long fibres.

REFERENCES

1. Sjöström, E. *Wood Chemistry, Fundamentals and Applications*, Academic Press, Inc., San Diego 1993.
2. Fengel, D. and Wegener, G. *Wood: Chemistry, Ultrastructure, Reactions*, Walter de Gruyter, Berlin 1989.
3. Gullichsen, J., in *Papermaking Science and Technology, Chemical Pulping 6A*, Edited by Gullichsen, J. and Fogelholm, C.-J., Fapet Oy, Jyväskylä 2000, Chapter 2.
4. Lai, Y.-Z., *Chemical Degradation*, in *Wood and Cellulosic Chemistry*, Edited by Hon, D.N.S. and Shiraishi, N., Marcel Dekker, Inc., New York, 2001, p. 443-512, and references therein.
5. Gellerstedt, G., *Pulping Chemistry*, in *Wood and Cellulosic Chemistry*, Edited by Hon, D.N.S. and Shiraishi, N., Marcel Dekker, Inc., New York, 2001, p. 859-905, and references therein.
6. Gierer, J. Lindeberg, O. and Norén, I., *Holzforschung* **33** (1979) 213-214.
7. Berthold, F., Lindfors, E.-L. and Gellerstedt, G., *Holzforschung* **52** (1998) 398-404.
8. Gierer, J. and Ljungren, S., *Svensk Papperstidn*. **82** (1979) 71-81.
9. Gierer, J., Ljungren, S., Ljunquist, P. and Norén, I., *Svensk Papperstidn*. **83** (1980) 75-82.
10. Miksche, G.E., *Acta Chem. Scand*. **26** (1972) 3275-3281.
11. Miksche, G.E., *Acta Chem. Scand*. **26** (1972) 4137-4142.
12. Kringstad, K.P. and Mörck, R., *Holzforschung* **37** (1983) 237-244.
13. Froass, P.M., Ragauskas, A.J. and Jiang, J., *J. Wood Chem. Technol*. **16** (1996) 347.
14. Karhunen, P. Mikkola, J., Pajunen, A. and Brunow, G., *Nord. Pulp Pap. Res. J.* **14** (1999) 123-128.
15. Agryropoulos, D.S., Jurasek, L., Krištofova, L., Xia, Z., Sun, Y. and Paluš, E., *J. Agric. Food Chem.* **50** (2002) 658-666.
16. Löwendahl, L. and Samuelson, O., *Svensk Papperstidn.* **80** (1977) 549-551.
17. Ahlgren, P., Ishizu, A., Szabo, I and Theander, O., *Svensk Papperstidn.* **71** (1968) 355.
18. Sinkey, J.D. and Thompson, N.S., *Pap. Puu* **56** (1974) 473-486.
19. Gierer, J. and Imsgard, F., *Svenk Papperstidn*. **80** (1977) 510-518.
20. Gierer, J., *Wood Sci. Technol*. **20** (1986) 1-33.
21. Gierer, J., *Holzforschung* **44** (1990) 387-394.
22. Asgari, F. and Argyropoulos, D.S., *Can. J. Chem*. **76** (1998) 1606-1615.
23. Ljungren, S. and Johanson, E., *Holzforschung* **44** (1990) 291-296.
24. Argyropoulos, D.S. and Liu, Y., *J. Pulp. Pap. Sci.* **26** (2000) 107-113.
25. Alén, R., in *Papermaking Science and Technology, Forest Products*, Edited by Stenius, P., Fapet Oy, Jyväskylä 2000, Chapter 2.
26. Yamasaki, T., Hosoya, S, Chen, C.L., Gratzl, J.S. and Chang, H.-M., *Int. Symp. Wood Pulp. Chem., Stockholm*, Vol. 2 (1981) 34-42.
27. Jiang, J., Chang, H.-M., Bhattacharjee, S.S. and Kwoh, D.L, *J. Wood Chem. Technol.* **7** (1987) 81-96.
28. Hortling, B., Tamminen, T., Tenkanen, M, Teleman, A. and Pekkala, O., *8th Int. Symp. Wood Pulp. Chem*., Helsinki, Vol. 1 (1995) 231-238.
29. Tenkanen, M., Tamminen, T. and Hortling, B., *Appl. Microbiol. Biotechnol*. **51** (1999) 241-248.
30. Fukagawa, N., Meshitsuka, G. and Ishizu, A., *J. Wood Chem. Technol*. **12** (1992) 425-445.
31. Eriksson, Ö., Goring, D.A and Lingren, B.O., *Wood Sci. Technol*. **14** (1980) 267-279.

32. Obst, J.R., *Tappi* **65** (1982) 109-112.
33. Gerasimowicz, W.V., Hicks, K. and Pfeffer, P., *Macromolecules* **17** (1984) 2597-2603.
34. Johnson, K.G. and Overend R.P., *Holzforschung* **45** (1991) 469-475.
35. Xie, Y., Yasuda, S., Wu, H. and Liu, H., *J. Wood Sci.* **46** (2000) 130-136.
36. Gierer, J. and Wännström, S., *Holzforschung* **38** (1984) 181.
37. Iversen, T. and Wännström, S., *Holzforschung* **40** (1986) 19-22.
38. Vikkula, A., Létumier, F., Tenkanen, M., Sipilä, J. and Vuorinen, T., *11th Int. Symp. Wood Pulp. Chem.*, Nice, Vol. 1 (2001) 51-54.
39. Košíková, B., Joniak, D. and Kosáková, *Holzforschung* **33** (1979) 11-14.
40. Taneda, H., Nakano, J., Hosoya, S. and Chang, H.-M., *J. Wood Chem. Technol*. **7** (1987) 485-498.
41. Sundquist, J., Rantanen, T. and Hovi, L., *Pap. Puu* **66** (1984) 252-257.
42. Gellerstedt, G. and Gustafsson, K., *J. Wood Chem. Technol*. **7** (1987) 65-80.
43. Jiang, Z.H. and Argyropoulos, D.S., *J. Pulp Pap. Sci*. **25** (1999) 25-29.
44. Gellerstedt, G., Heuts, L. and Robert, D., *J. Pulp Pap. Sci*. **25** (1999) 111-117.
45. Ahvazi, B. C.; Pageau, G.; Argyropuolos, D.S., *Can. J. Chem*. **76** (1998) 506-512.
46. Gellerstedt, G. and Heuts, L. *J. Pulp Pap. Sci*. **23** (1997) J335-J340.
47. Akim, L.G., Colodette, J.L. and Argyropoulos, D.S., *Can. J. Chem*. **79** (2001) 201-210.
48. Tohmura, S.I. and Argyropoulos, D.S., *J. Agric. Food Chem.* **49** (2001) 536-542.
49. Gierer, J. and Lindeberg, O., *Acta Chem. Scand.* **B33** (1979) 580-622.
50. Lai, Y.-Z., Funaoka, M. and Chen, H.-T., *Holzforschung* **48** (1994) 355-359.
51. Saka, S. and Goring, D.A.I., In *Biosynthesis and Biodegradation of Wood Components*, Ed. Higuchi, T., Academic Press, Inc., Orlando, 1985, Chapter 3, p. 51-62.
52. Hardell, H.-L., Leary, G., Stoll, M. and Westermark, U., *Svensk Papperstidn*. **83** (1980) 44-48.
53. Boutelje, J. and Eriksson, I., *Holzforschung* **38** (1984) 249-252.
54. Sorvari, J., Sjöström, E., Klemola, A. and Laine, J.E., *Wood Sci. Technol*. **20** (1986) 35-51.
55. Chen, H.T., Funaoka, M. and Lai, Y.-Z., *Wood Sci. Technol*. **31** (1997) 433-440.
56. Westermark, U. and Samuelsson, B., *Holzforschung* **40** (1986) 139-146.
57. Heijnesson, A., Simonson, R. and Westermark, U., *Holzforschung* **49** (1995) 313-318.
58. Heijnesson-Hultén, A., Simonson, R., and Westermark, U., *Pap. Puu*, **79** (1997) 411-415.
59. Laine, J., Stenius, P., Carlson, G. and Ström, G., *Cellulose* **1** (1994) 145-160.
60. Hortling, B., Tamminen, T. and Pekkala, O., *Tappi Pulping Conference*, Nashville, Vol. 1 (1996) 189-196.
61. Hortling, B., Tamminen, T. and Turunen, E., *9th Int. Symp. Wood Pulp. Chem.*, Montreal, Vol. 2 (1997) B6 - 1-B6-4.
62. Westermark, U. and Capretti, G., *Nord. Pulp. Pap. Res. J.* **3** (1988) 95-99.
63. Atalla, R.H., Gast, J.C., Sindorf, D.W., Bartuska, V.J. and Maciel, G.E., *J. Am. Chem. Soc.* **102** (1980) 3249-3251.
64. Earl, W.L. and VanderHart, D.L., *J. Am. Chem. Soc*. **102** (1980) 3251-3252.
65. Earl, W.L. and VanderHart, D.L., *Macromolecules* **14** (1981) 570.
66. Maciel, G.E., Kolodziejski, W.L., Bertran, M.S. and Dale, B.E., *Macromolecules* **15** (1982) 686.
67. Horii, F., Hirai, A. and Kitamaru, R., *Polymer Bull.* **8** (1982) 163-170.

68. VanderHart, D.L. and Atalla, R.H., *Macromolecules* **17** (1984) 1465-1472.
69. Larsson, P.T., Wickholm, K. and Iversen T., *Carbohydr. Res*. **302** (1997) 19-25.
70. Newman, R.H. and Hemmingson, J.A, *Cellulose* **2** (1994) 95-110.
71. Newman, R.H., *Holzforschung* **52** (1998) 157-159.
72. Wickholm, K., Larsson, P.T. and Iversen, T., *Carbohydr. Res.* **312** (1998) 123-129.
73. Larsson, P.T., Hult, E-L., Wickholm, K., Pettersson, E. and Iversen, T., *Solid State NMR* **15** (1999) 31-40.
74. Wickholm, K., *Structural Elements in Native Celluloses*, Doctoral Thesis, Royal Institute of Technology, Stockholm, 2001.
75. Teeäär, R, Serimaa, R, and Paakkari, T., *Polym. Bull*. **17** (1987) 231-237.
76. Horii, F., Hirai, A. and Kitamaru, R., *J. Carbohydr. Chem*. **3** (1984) 641-662.
77. Hult, E.-L., Larsson, P.T. and Iversen, T., *Cellulose* **7** (2000) 35-55.
78. Newman, R.H. and Hemmingson, J.A., *Holzforschung* **44** (1990) 351-355.
79. Mitikka-Eklund, M., *Sorption of Xylans on Cellulose Fibres*, Licentiate Thesis, University of Jyväskylä, 1996.
80. Marchessault, R.H., Taylor, M.G and Winter, W.T., *Can. J. Chem*. **68** (1990) 1192-1195.
81. Teleman, A., Larsson, P.T. and Iversen, T., *Cellulose* **8** (2001) 209-215.
82. Newman, R.H., *J. Wood Chem. Technol*. **14** (1994) 451-466.
83. Kim, Y.S. and Newman, R.H., *Holzforschung* **49** (1995) 109-114.
84. Newman, R.H., Hemmingson, J.A. and Suckling, I.D., *Holzforschung* **47** (1993) 234-238.
85. Wickholm, K., Hult, E-L., Larsson. P.T., Iversen, T. and Lennholm, H., *Cellulose* **8** (2001) 139-148.
86. Newman, R.H., *Solid State NMR* **15** (1999) 21-29.
87. Lopes, M.H., Saryachev, A., Pascoal Neto, C. and Gil, A.M., *Solid State NMR* **16** (2000) 109-121.
88. Horii, F., Hirai, A. and Kitamaru, R., *Macromolecules* **20** (1987) 2117-2120.
89. Sugiyama, J., Vuong, R. and Chanzy, H., *Macromolecules* **24** (1991) 4168-4175.
90. Sugiyama, J., Persson, J. and Chanzy, H., *Macromolecules* **24** (1991) 2461-2466.
91. Debzi, E.M., Chanzy, H., Sugiyama, J., Tekely, P and Excoffier, G., *Macromolecules* **24** (1991) 6816-6822.
92. Yamamoto, H. and Horii, F., *Macromolecules* **26** (1993) 1313-1317.
93. Lennholm, H. and Iversen, T., *Holzforschung* **49** (1995) 119-126.
94. Kuga, S., Takagi, S. and Brown, R.M. Jr, *Polymer* **34** (1993) 3293-3297.
95. Shibazaki, H., Saito, M., Kuga, S. and Okano, T., *Cellulose* **5** (1998) 165-173.
96. Ferrige, A.G. and Lindon, J.C., *J. Magn. Reson*. **31** (1978) 337-340.
97. Cael, J. J., Kwoh, D.L.W., Bhattacharjee, S.S. and Patt, S., *Macromolecules* **18** (1985) 819-821.
98. Belton, P.S., Tanner, S.F, Cartier, N. and Chanzy, H., *Macromolecules* **18** (1989) 1615-1617.
99. Newman, R.H., *Cellulose* **4** (1997) 269-279.
100. Lennholm, H., Larsson, T. and Iversen, T., *Carbohydr. Res.* **261** (1994) 119-131.
101. Lennholm, H., Wallbäcks, L. and Iversen, T., *Nord. Pulp Pap. Res. J.* **10** (1995) 46-50.
102. Ha, M.A., Apperley, D., Evand, B.W., Huxham, I.M., Jardine, W.G., Vietor, R.J., Reis, D., Vian, B. and Jarvis, M.C., *Plant J.* **16** (1998) 183-190.
103. Heux, L., Dinand, E. and Vignon, M.R., *Carbohydr. Polym*. **40** (1999) 115-124.
104. Hult, E.L., Larsson, T. and Iversen, T., *Polymer* **42** (2001) 3309-3314.

105. Newman, R.H., *Carbon-13 NMR Studies of Lignin in Solid Samples – a Review*, Chemistry Division Report, DSIR, New Zealand, 1989.
106. Leary, G.J. and Newman, R.H., In *Methods in Lignin Chemistry*, Ed. By Lin, S.Y. and Dence, C.W., Springer-Verlag, Berlin, 1992, Chapter 4.5, p. 146-161.
107. Robert, D., In *Methods in Lignin Chemistry*, Ed. By Lin, S.Y. and Dence, C.W., Springer-Verlag, Berlin, 1992, Chapter 5.4.
108. Opella, S.J. and Frey, M.H., *J. Am. Chem. Soc*. **101** (1979) 5854-5856.
109. Manders, W.F., *Holzforschung* **41** (1987) 13-18.
110. Hawkes, G.E., Smith, C.Z., Utley, J.H.P., Vargas, R.R. and Viertler, H., *Holzforschung* **47** (1993) 302-312.
111. Hatcher, P.G., *Org. Geochem.* **11** (1987) 31-39.
112. Bates, A.L. and Hatcher, P.G., *Org. Geochem*. **18** (1992) 407-416.
113. Attalla, M.I., Serra, R.G., Vassallo, A.M. and Wilson, *Org. Geochem*. **12** (1988) 235-244.
114. Alemany, L.B., Grant, D.M., Alger, T.D., and Pugmire, R.J., *J. Am. Chem. Soc*. **105** (1983) 6697-6704.
115. Fyfe, C.A., *Solid State NMR for Chemists*, C.F.C Press, Ontario, 1983.
116. Argyropoulos, D.S., Morin, F.G. and Lapcik, L., *Holzforschung* **49** (1995) 115-118.
117. Ahvazi, B.C. and Argyropoulos, D.S., *Solid State NMR* **15** (1999) 49-57.
118. Ahvazi, B. and Argyropoulos, D.S, *Wood. Sci. Technol*. **34** (2000) 45-53.
119. Košiková, B., Hricovíni, and Cosentino, C., *Wood Sci. Technol*. **33** (1999) 373-380.
120. Schenk, W., Reichert, D. and Schneider, H., *Polymer* **31** (1990) 329-335.
121. Bielecki, A., Burum, D.P., Rice, D.M. and Karasz, F.E., *Macromolecules* **24** (1991) 4820-4822.
122. White, J.L., Dias, A.J. and Ashbaugh, J.R., *Macromolecules* **31** (1998) 1880-1888.
123. White, J.L. and Mirau, P.A., *Macromolecules* **27** (1994) 1648-1650.
124. Kilpeläinen, I., Ämmälahti, E., Brunow, G. and Robert, D., *Tetrahedron Lett*. **49** (1994) 9267-9270.
125. Brunow, G., Ämmälahti, E., Niemi, T., Sipilä, J., Simola, L.K. and Kilpeläinen, I., *Phytochem.* **47** (1998) 1495-1500.
126. Ämmälahti, E., Brunow, G., Bardet, M. Robert, D. and Kilpeläinen, I., *J. Agric. Food Chem.* **46** (1998) 5113-5117.
127. Ralph, J., Marita, J.M., Ralph, S., Hatfield, R.D., Lu, F., Ede, R.M., Peng, J., Quideau, S., Helm, R.F., Grabber, J.H., Kim, H., Jimenez-Monteon, G., Zhang, Y., Jung, H-J. G., Landucci, L.L., MacKay, J.J., Sederoff, R.R., Chapple, C. and Boudet, A.M., In *Advances in Lignocellulosics Characterization*, Ed. By Argyropoulos, D.S., Tappi Press, Atlanta, 1999, Chapter 3, p. 55-108.
128. Friebolin, H., *Basic One- and Two-Dimensional NMR Spectroscopy*, 3rd Ed., Wiley-VCH, Darmstadt, 1998.
129. Wijmenga, S.S., Hallenga, K. and Hilbers, C.W., *J. Magn. Res.* **84** (1989) 634-642.
130. Hattula, T., *Pap. Puu* **68** (1986) 926-931.
131. Evans, R., Newman, R.H., Roick, U.C., Suckling, I.D. and Wallis, A.F.A., *Holzforschung* **49** (1995) 498-504.
132. Newman, R.H. and Hemmingson, J.A., *8th Int. Symp. Wood Pulp. Chem*., Helsinki, 1995, Vol.1. 519-525.
133. Liitiä, T., Maunu, S.L., Pekkala, O., Varhimo, A. and Hortling, B., To be published in the *7th European Workshop on Lignocellulosics and Pulp*, Turku, August 26-29, 2002.
134. Hattula, T., *Pap. Puu* **69** (1987) 92-95.

135. Tamminen, T. and Hortling, B., *11th Int. Symp. Wood Pulp. Chem.*, Nice, 2001, Vol. 1, p. 297-300.
136. Lennholm, H. and Iversen, T., *Nord. Pulp Pap. Res. J.* **10** (1995) 104-109.
137. Leary, G.J., Morgan, K.R. and Newman, R.H., *Holzforschung* **40** (1986) 221-224.
138. Hu, X.-P. and Hsieh, Y.-L., *J. Polym. Sci. Part B* **34** (1996) 1451-1459.
139. Hult, E.L., *CP/MAS ^{13}C-NMR Spectroscopy Applied to Structure and Interaction Studies on Wood and Pulp Fibers*, Ph.D. Thesis, Royal Institute of Technology, Stockholm, 2001.
140. Wormald, P., Wickholm, K., Larsson, P.T. and Iversen, T., *Cellulose* **3** (1996) 141-152.
141. De Souza, I.J., Bouchard, J., Methot, M., Berry, R. and Argyropulos, D.S., *Int. Pulp Bleach. Conf.*, Halifax, Canada, June 27-30, 2000, p. 41-45.
142. Tamminen, T.;Hortling, B., *Isolation and Cheracterization of Residual Lignin*. In *Advances in Lignocellulosic Characterization*, Argyropoulus, D., Ed., Tappi Press: Atlanta, 1999, pp. 1-42.
143. Gierer, J.; Pettersson, I.; Smedman, L.-Å.; Wennberg, I., *Acta Chem. Scand*. 27, (1973) 2083-2094.
144. Pham, Q.-T.; Petiaud, R.;Waton, H. *Proton and Carbon NMR Spectra of Polymers*, Vol. II, John Wiley & Sons, 1983, p. 334-336.
145. Whiting, P. and Goring, D.A.I., *Svensk Papperstidn*. **84** (1981) R120-122.
146. Maurer, A. and Fengel, D., *Holzforschung* **46** (1991) 417-423.
147. Terashima, N., Fukushima, K. and Imai, T., *Holzforshug* **46** (1992) 271-275.
148. Kolodziejski, W., Frye, J.S. and Maciel, G.E., *Anal. Chem.* **54** (1982) 1419-1424.

APPENDIX 1

Production of the ECF-bleached FT-Kraft, Kraft and PS-AQ pulps

Table 1. *Pulping conditions.*

	FT-Kraft	Kraft	PS-AQ
Liquor to wood ratio (l/kg)	-	3.5	3.5
Liquor flow (ml/min)	700	-	-
Effective alkali (mol/kg)	-	4.5	4.5
Effective alkali (mol/l)	0.5	-	-
Sulphidity (%)	35	35	19.9
PS dose (g/kg wood)	-	-	12
AQ dose (g/kg wood)	-	-	1

Cooking temperature was 170ºC for pine and 160ºC for birch. The kappa number of pine and birch pulps was 30 and 20, respectively.

Table 2. *ECF-bleaching conditions.*

Stage	O	D_0	(EO)	D_1	N	D_2
Pulp charge g (o.d)	1750	845	1690	840	-	830
Consistency (%)	12	9	12	9	3	9
Temperature (ºC)	90	55	67	65	65	70
Time (min)	75	60	60	180	2	180
O_2 pressure (bar)	8	-	3	-	-	-
NaOH (% on pulp)	1.65-2.7	-	-	-	-	-
$MgSO_4$ (% on pulp)	0.5	-	-	-	-	-
Final pH	-	2.1-2.3	11	3.5	10	4.1-4.6
Act. Cl multible	-	0.19	-	0.4-0.45	-	-

Table 3*. Properties of ECF-bleached pine and birch pulps.*

	Kappa number	Brightness, ISO (%)	Viscosity (ml/g)	Pulp yield on wood (%)
Pine:				
FT-Kraft	0.6	89.7	870	42
Kraft	0.7	89.4	990	44.1
PS-AQ	0.6	89.3	1000	47
Birch:				
FT-Kraft	0.8	91.5	1170	49.6
Kraft	0.7	90.8	1200	51.4
PS-AQ	0.8	90.2	1220	53.7

Table 4. *Total monosaccharides (mg/100mg) and monosaccharide composition (%).*

	HH_{tot} (mg/100mg)	Ara (%)	Gal (%)	Glu (%)	Xyl (%)	Man (%)
Pine:						
FT-Kraft	100.3	0.3	+	88.2	5.8	5.7
Kraft	98.5	0.8	0.3	84.3	8.1	6.5
PS-AQ	95.8	0.8	0.5	81.7	7.3	9.7
Birch:						
FT-Kraft	93.8	-	-	78	22	+
Kraft	96.7	-	-	75.4	24.6	-
PS-AQ	92.5	-	-	73.3	26.7	+

APPENDIX 2

Isolation of residual lignin-carbohydrate complexes

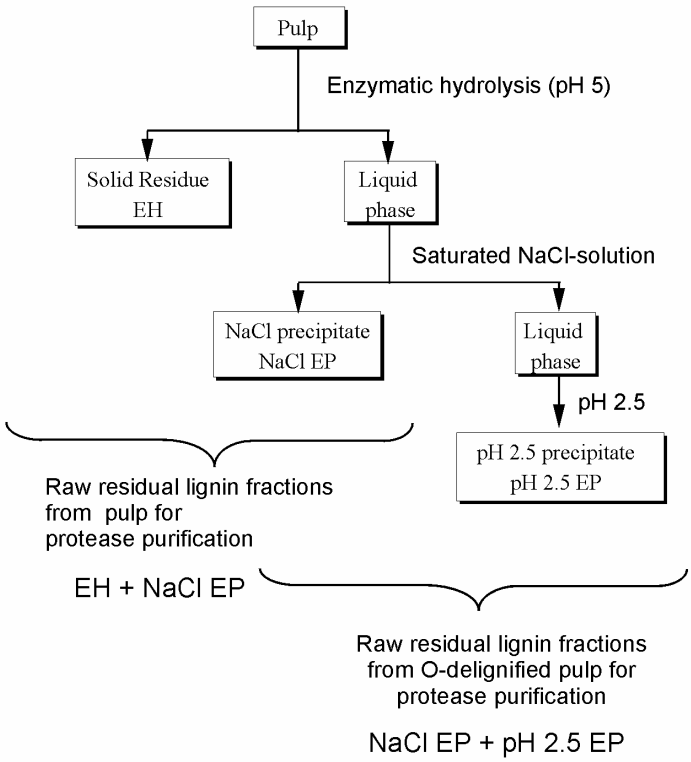

Purification of the enzymatic hydrolysis fractions